Cell Reports
Medicine

Article

Probiotics and their metabolite spermidine enhance IFN-γ^+CD4$^+$ T cell immunity to inhibit hepatitis B virus

Graphical abstract

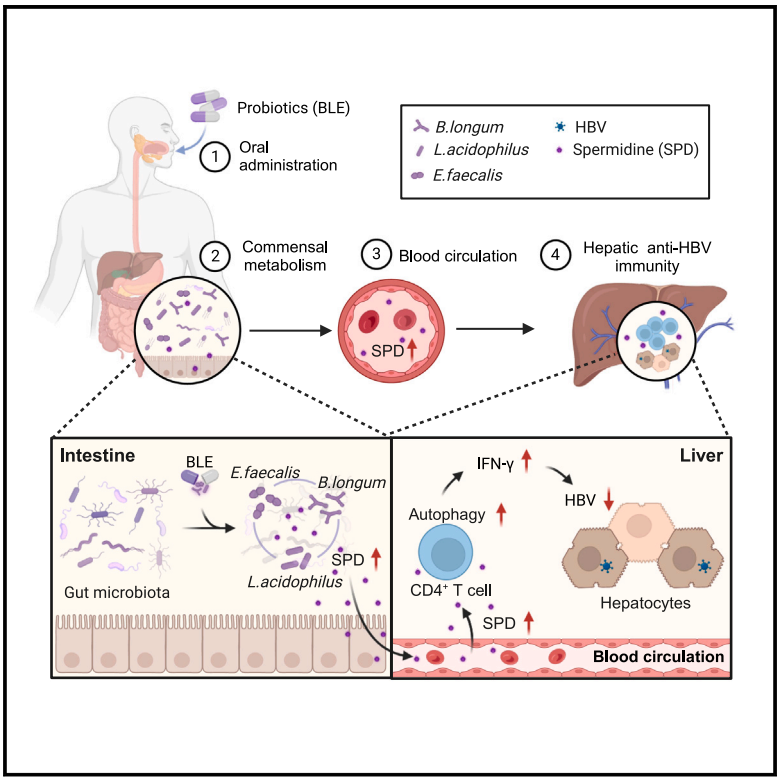

Highlights

- Probiotics promote HBV clearance by producing spermidine
- Probiotics and spermidine enhance IFN-γ^+CD4$^+$ T cell function through autophagy
- Probiotics induce the decline of serum HBsAg in patients with low HBsAg levels

Authors

Tixiao Wang (王体潇), Yuchen Fan (范玉琛), Siyu Tan (谭思雨), ..., Xiaohong Liang (梁晓红), Chunyang Li (李春阳), Chunhong Ma (马春红)

Correspondence

liangxiaohong@sdu.edu.cn (X.L.), lichunyang@sdu.edu.cn (C.L.), machunhong@sdu.edu.cn (C.M.)

In brief

Commensal microbes are promising in the functional cure of HBV infection. Wang et al. demonstrate that probiotics and their metabolite spermidine effectively promote the decline of HBsAg and inhibit HBV replication via autophagy-enhanced IFN-γ^+CD4$^+$ T cell immunity, highlighting the therapeutic potential of probiotics and spermidine for the functional cure of HBV patients.

Wang et al., 2024, Cell Reports Medicine 5, 101822
November 19, 2024
https://doi.org/10.1016/j.xcrm.2024.101822

CellPress

Cell Reports Medicine

CellPress
OPEN ACCESS

Article

Probiotics and their metabolite spermidine enhance IFN-γ^+CD4$^+$ T cell immunity to inhibit hepatitis B virus

Tixiao Wang (王体潇),[1,8] Yuchen Fan (范玉琛),[3,8] Siyu Tan (谭思雨),[2] Zehua Wang (王泽华),[2] Mengzhen Li (李梦真),[2] Xiaowei Guo (郭小维),[2] Xiangguo Yu (于祥国),[2] Qinghai Lin (林清海),[2] Xiaojia Song (宋晓佳),[2] Leiqi Xu (徐蕾琪),[4] Lixiang Li (李理想),[4] Shiyang Li (李石洋),[5] Lifen Gao (高立芬),[2] Xiaohong Liang (梁晓红),[2,*] Chunyang Li (李春阳),[6,*] and Chunhong Ma (马春红)[2,7,9,*]

[1]Department of Endocrinology and Metabolism and Department of Immunology, Qilu Hospital, School of Basic Medical Sciences, Cheeloo College of Medicine, Shandong University, Jinan, Shandong 250012, China
[2]Key Laboratory for Experimental Teratology of Ministry of Education, Department of Immunology, School of Basic Medical Sciences, Qilu Hospital, Cheeloo College of Medicine, Shandong University, Jinan, Shandong 250012, China
[3]Department of Hepatology, Qilu Hospital of Shandong University, Jinan, Shandong 250012, China
[4]Department of Gastroenterology, Qilu Hospital of Shandong University, Jinan, Shandong 250012, China
[5]Advanced Medical Research Institute, Shandong University, Jinan, Shandong 250012, China
[6]Key Laboratory for Experimental Teratology of Ministry of Education, Department of Histology and Embryology, School of Basic Medical Sciences, Cheeloo College of Medicine, Shandong University, Jinan, Shandong 250012, China
[7]School and Hospital of Stomatology, Cheeloo College of Medicine, Shandong University, Jinan, Shandong 250012, China
[8]These authors contributed equally
[9]Lead contact
*Correspondence: liangxiaohong@sdu.edu.cn (X.L.), lichunyang@sdu.edu.cn (C.L.), machunhong@sdu.edu.cn (C.M.)
https://doi.org/10.1016/j.xcrm.2024.101822

SUMMARY

The therapeutic potential of commensal microbes and their metabolites is promising in the functional cure of chronic hepatitis B virus (HBV) infection, which is defined as hepatitis B surface antigen (HBsAg) loss. Here, using both specific-pathogen-free and germ-free mice, we report that probiotics significantly promote the decline of HBsAg and inhibit HBV replication by enhancing intestinal homeostasis and provoking intrahepatic interferon (IFN)-γ^+CD4$^+$ T cell immune response. Depletion of CD4$^+$ T cells or blockage of IFN-γ abolishes probiotics-mediated HBV inhibition. Specifically, probiotics-derived spermidine accumulates in the gut and transports to the liver, where it exhibits a similar anti-HBV effect. Mechanistically, spermidine enhances IFN-γ^+CD4$^+$ T cell immunity by autophagy. Strikingly, administration of probiotics in HBV patients reveals a preliminary trend to accelerate the decline of serum HBsAg. In conclusion, probiotics and their derived spermidine promote HBV clearance via autophagy-enhanced IFN-γ^+CD4$^+$ T cell immunity, highlighting the therapeutic potential of probiotics and spermidine for the functional cure of HBV patients.

INTRODUCTION

Globally, approximately 296 million people are chronically infected with hepatitis B virus (HBV), which poses a high risk of liver cirrhosis and hepatocellular carcinoma, making it as one of the most serious common infectious agents.[1] In 2016, the World Health Organization called for the goal of eliminating viral hepatitis, defined as 95% reduction in HBV incidence and 65% reduction in mortality by 2030.[2,3] The ideal goal of antiviral treatment for HBV patients is to achieve a functional cure, which is characterized by the persistent suppression of HBV DNA and the loss of serum hepatitis B surface antigen (HBsAg).[4,5] Unfortunately, achieving the functional cure for chronic HBV infection is difficult. The natural history has a success rate of less than 1%, and current antiviral drugs yield no more than 5% success rate even after long-term treatment.[6,7] Dysfunctional or exhausted T cells have been demonstrated to restrict the strength of HBV clearance, and recovery of T cell immunity is believed to be the most promising strategy for functional cure.[8] Stimulating T cell co-stimulatory molecule OX40 and blockade of programmed cell death ligand 1 (PD-L1) synergistically promote the functional restoration of HBV-specific CD4$^+$ T cells, leading to the production of interferon (IFN)-γ and interleukin (IL)-21, which are essential for HBV clearance.[9] Hoogeveen et al. also showed that functional cure is associated with robust responses by HBV-specific CD4$^+$ T cells.[10] Therefore, it is important to develop exact and effective treatment strategies for restoring dysfunctional T cell immunity and achieve functional cure of HBV infection.

The liver is the unique target organ that orchestrates HBV-mediated immune response and is coordinated by gut microbe-derived ligands or metabolites through the gut-liver axis.[11] Altered and flexible profile of gut microbiota in HBV infection has been

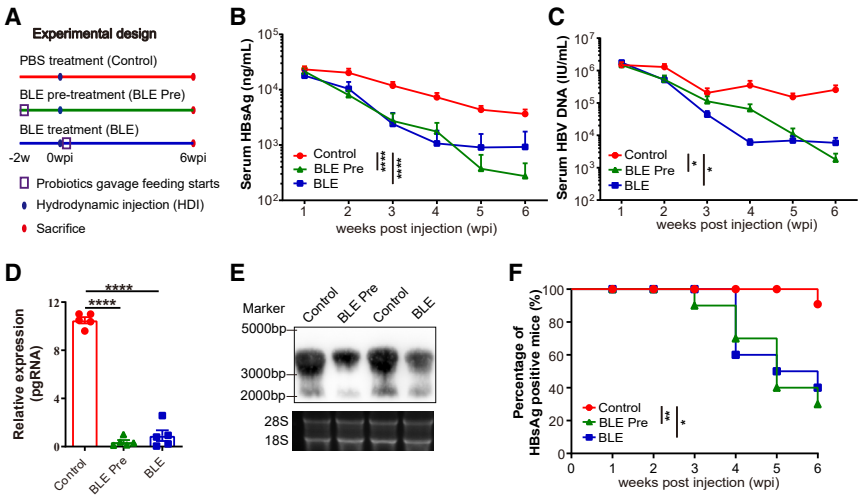

Figure 1. Supplementation with BLE promoted HBV clearance in mice

(A) Study design: male five-week-old C57BL/6J mice were hydrodynamically injected with 6 μg of AAV/HBV1.2 plasmid and gavage fed with probiotics (BLE, PBS as control) daily starting two weeks before (Pre) or at 3 dpi of HDI (control, $n = 10$; BLE Pre, $n = 10$; BLE, $n = 10$).

(B–E) Levels of serum HBsAg (B), HBV DNA (C), hepatic pgRNA (D), and HBV RNA (E) were detected by ELISA, qPCR, and northern blot, respectively.

(F) The percentages of HBsAg-positive mice (HBsAg > 1 ng/mL) at the indicated time points were calculated.

Data were expressed as mean ± SEM. The statistical tests were performed by two-way analysis of variance (ANOVA) with Dunnett's multiple comparison test (B and C), t test (D), or log rank (F). *$0.01 < p$ value < 0.05; **$0.001 < p$ value < 0.01; ****p value < 0.0001.

reported,[12–14] and the establishment of gut microbiota determines the age-related HBV clearance, in which T cell response plays pivotal roles.[15,16] In the limited data of HBV patients, Ren et al. reported that fecal microbiota transplantation (FMT) presented the ability to induce the decline of HBV e-antigen (HBeAg) expression in persistent HBeAg-positive patients even after long-term antiviral treatment.[17] Mechanistically, commensal microbes and their metabolites regulate the production of IL-22, IL-17A, and IL-21 to promote intestinal immune homeostasis.[18,19] However, multidrug-resistant organisms colonized in healthy donors' feces during donation activities would pose a risk for FMT.[20] Probiotics are widely used as a food supplement to assist in the treatment of many health or disease conditions.[21] Currently, the molecular and immune mechanism by which probiotics promote HBV clearance remains unclear. Consequently, the key and specific microbes or metabolites that facilitate HBV clearance have yet to be identified.

Here, we reported that probiotics (*B. longum*, *L. acidophilus*, and *E. faecalis*, BLE), widely used in clinical practice, promote HBV clearance in both specific-pathogen-free (SPF) mice and germ-free (GF) mice. Specifically, spermidine (SPD) derived from accumulated probiotics in the gut could transport to the liver and exhibit a similar anti-HBV effect to probiotics. Mechanistically, depletion of $CD4^+$ T cells or blockage of IL-21R or IFN-γ almost completely dampened probiotics-induced HBV inhibition, and SPD administration activated the $CD4^+$ T cell immunity through autophagy. In HBV patients undergoing antiviral treatment, probiotics showed the potential to induce the decline of serum HBsAg.

RESULTS

Administration of probiotics BLE promotes HBV clearance and improves intestinal commensal homeostasis and barrier function

To evaluate the efficiency of probiotics (BLE) in HBV clearance, HBV-carrier mouse models were prepared by hydrodynamical injection (HDI) of adeno-associated virus/HBV1.2 (AAV/HBV1.2) plasmids in 5-week-old C57BL/6 mice.[22] BLE were administered by gavage daily starting from either 2 weeks prior to HDI (BLE Pre group) or after 3 days post injection (BLE group) (Figure 1A). As shown in Figures 1B–1E, both BLE and BLE Pre significantly inhibited HBV replication, displayed as decreased levels of serum HBsAg, HBV DNA, as well as hepatic pregenomic RNA (pgRNA) and HBV RNA. Consistently, BLE administration significantly decreased the percentage of HBsAg-positive mice within 6 weeks post injection (wpi) (Figure 1F). In addition, no liver injury was detected in mice treated with BLE (Figures S1A and S1B). Since BLE and BLE Pre showed similar anti-HBV effects, we used orally daily administration of BLE as the routine probiotic treatment in the following experiments.

Probiotics show well-defined improvement in gut microbiota. We then investigated the effect of BLE administration on microbiota profile in HBV-carrier mice. Principal coordinate analysis (PCoA) revealed significant shifts ($p = 0.004$) in intestinal microbiome composition between control and BLE mice (Figure 2A). Taxonomic alpha diversity (Chao diversity) analysis showed a marked increase in species richness in BLE groups (Figure 2B). Moreover, linear discriminant analysis effect size (LEfSe) analysis displayed that the microbiome of BLE mice was significantly enriched with families *Prevotellaceae*, *Clostridiaceae*, *Akkermansia*, and *Ruminococcaceae* (Figure 2C), which have been suggested to contribute to the restoration of exhausted $CD8^+$ T cell mediated by anti-PD-1 or CTLA-4 antibodies.[23–25] Further, qPCR analysis using bacterium-specific primers showed that the abundance of BLE in the feces significantly increased after probiotics supplementation, suggesting the accumulation of probiotics bacteria (Figure 2D).

Intestinal microbiota plays a critical role in maintaining gut barrier and permeability, which is strongly associated with the development of chronic liver diseases.[26] In accordance, we detected lower serum fluorescein isothiocyanate (FITC)-dextran concentration in BLE mice than in control mice (Figure S1C), indicating improved intestinal barrier integrity in BLE mice. Consistently, the serum level of intestinal fatty acid binding protein (iFABP), a biomarker of enterocyte damage,[27] significantly decreased in BLE mice (Figure S1D). In contrast, there was

CellPress
OPEN ACCESS

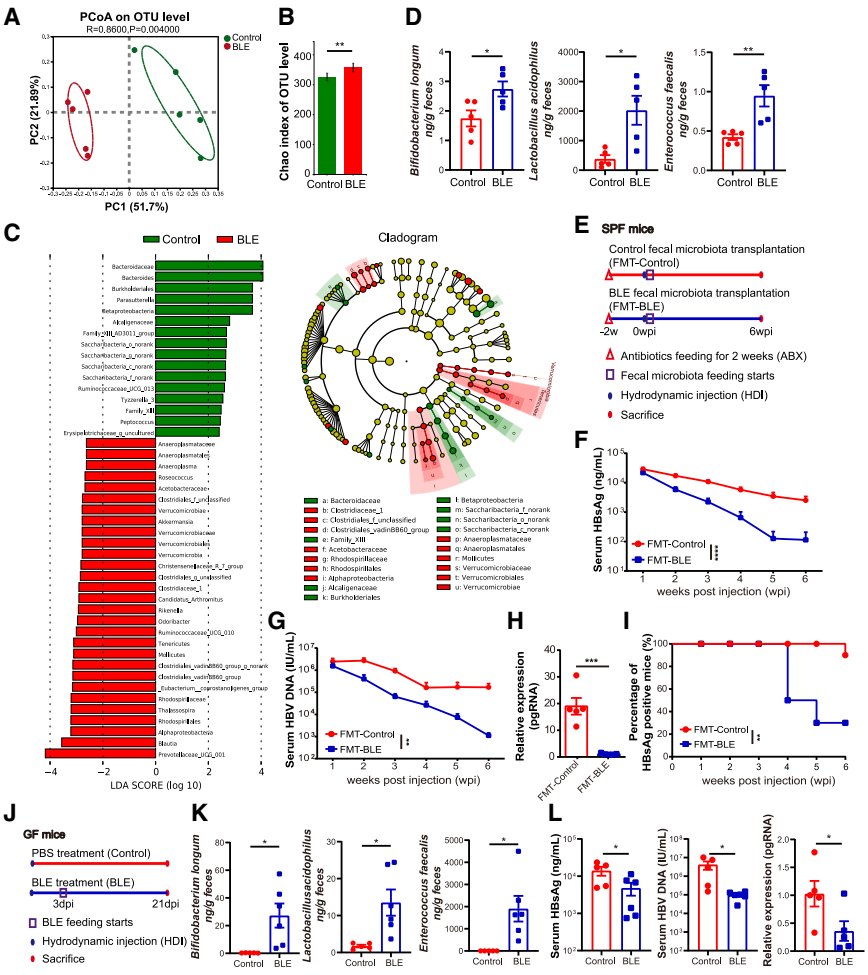

Figure 2. Accumulation of BLE contributed to gut microbiota homeostasis and HBV clearance

(A–C) 16S rRNA sequencing was performed with feces collected at 2 wpi. Beta diversity comparison via PCoA analysis (A) and alpha diversity comparison via Chao index analysis (B) showed a difference between the two groups. Bray-Curtis distance algorithm was used for PCoA analysis. (C) LEfSe (linear discriminant analysis effect size) predictions for bacterial families found in fecal pellets of control (green) and BLE (red) mice were shown, with cutoffs of LDA < −2 or LDA > 2.

(D) Fecal bacterial genomic DNA was extracted from control and BLE mice. The expression of *B. longum*, *L. acidophilus*, and *E. faecalis* was determined by qPCR.

(E) Study design: male three-week-old C57BL/6J mice were treated with antibiotics water for two weeks and then hydrodynamically injected with 6 μg of pAAV/HBV1.2 plasmid and fed with fecal microbiota from control and BLE mice daily starting at 3 dpi of HDI (FMT-control, $n = 10$; FMT-BLE, $n = 10$).

(F–H) Levels of serum HBsAg (F), HBV DNA (G), and hepatic pgRNA (H) were detected by ELISA and qPCR.

(I) The percentages of HBsAg-positive mice (HBsAg > 1 ng/mL) at the indicated time points were calculated.

(J) Study design: male six-week-old C57BL/6J GF mice were hydrodynamically injected with 6 μg of pAAV/HBV1.2 plasmid and gavage fed with BLE daily starting at 3 dpi of HDI.

(K) The expression of *B. longum*, *L. acidophilus*, and *E. faecalis* was determined by qPCR.

(L) Levels of serum HBsAg, HBV DNA, and hepatic pgRNA were detected by ELISA and qPCR.

Data were expressed as mean ± SEM. The statistical tests were performed by analysis of similarities (ANOSIM) (A), t test (B, D, H, K, and L), parametric factorial Kruskal-Wallis (KW) sum-rank test (C), two-way ANOVA (F and G), or log rank (I). *0.01 < p value < 0.05; **0.001 < p value < 0.01; *** 0.0001 < p value < 0.001; ****p value < 0.0001.

higher expression of tight junction proteins, including *Claudin 1*, *Occludin*, and *Tjp1*, in small intestine (SI) tissues from BLE mice than those from control mice (Figure S1E).

It has been well documented that microbiota induces the production of IL-17A, IL-21, and IL-22 to improve gut integrity and homeostasis.[18,19] As expected, significantly higher expression of IL-17A, IL-21, and IL-22 at both the mRNA and protein levels was detected in SI tissues from BLE mice (Figures S1F and S1G). Flow cytometric (FCM) analysis verified the marked increase in the frequency of T cells producing IL-17A, IL-21, and IL-22 in lymphocytes of small intestinal lamina propria, mesenteric lymph nodes (mLNs) and Peyer's patches (PPs) from BLE mice than control mice (Figures S1H–S1K). Collectively, these data suggest that accumulation of BLE improves intestinal commensal homeostasis and barrier functions in HBV-carrier mice.

Accumulation of BLE contributes to HBV clearance in mice

To assess whether gut microbiota is involved in BLE-mediated HBV suppression, feces were collected from PBS- or BLE-treated HBV-carrier mice (donor mice). Then, FMT experiments were performed with recipient mice, which were gut-sterilized using a 14-day antibiotic mixture (ABX) treatment followed by HDI of HBV at the age of 5 weeks (Figure 2E). As shown in Figures 2F–2H, transplantation of fecal microbiota from BLE mice (FMT-BLE) greatly promoted HBV clearance in recipient mice, displaying obviously decreased levels of serum HBsAg and HBV DNA and reduced hepatic pgRNA expression when compared to mice that received control fecal microbiota (FMT-Control). Similarly, the percentage of HBsAg-positive mice in FMT-BLE mice was significantly lower than that in FMT-Control mice (Figure 2I).

To further validate the direct role of BLE in HBV clearance, we included GF mice to establish a HBV model by HDI, followed by probiotics administration (Figure 2J). Consisting with results in SPF mice, supplementation with BLE largely increased the numbers of BLE in the feces from GF mice (Figure 2K) and decreased levels of serum HBsAg, HBV DNA, and hepatic pgRNA (Figure 2L). Taken together, these data suggest that the accumulation of BLE contributes to HBV clearance in mice.

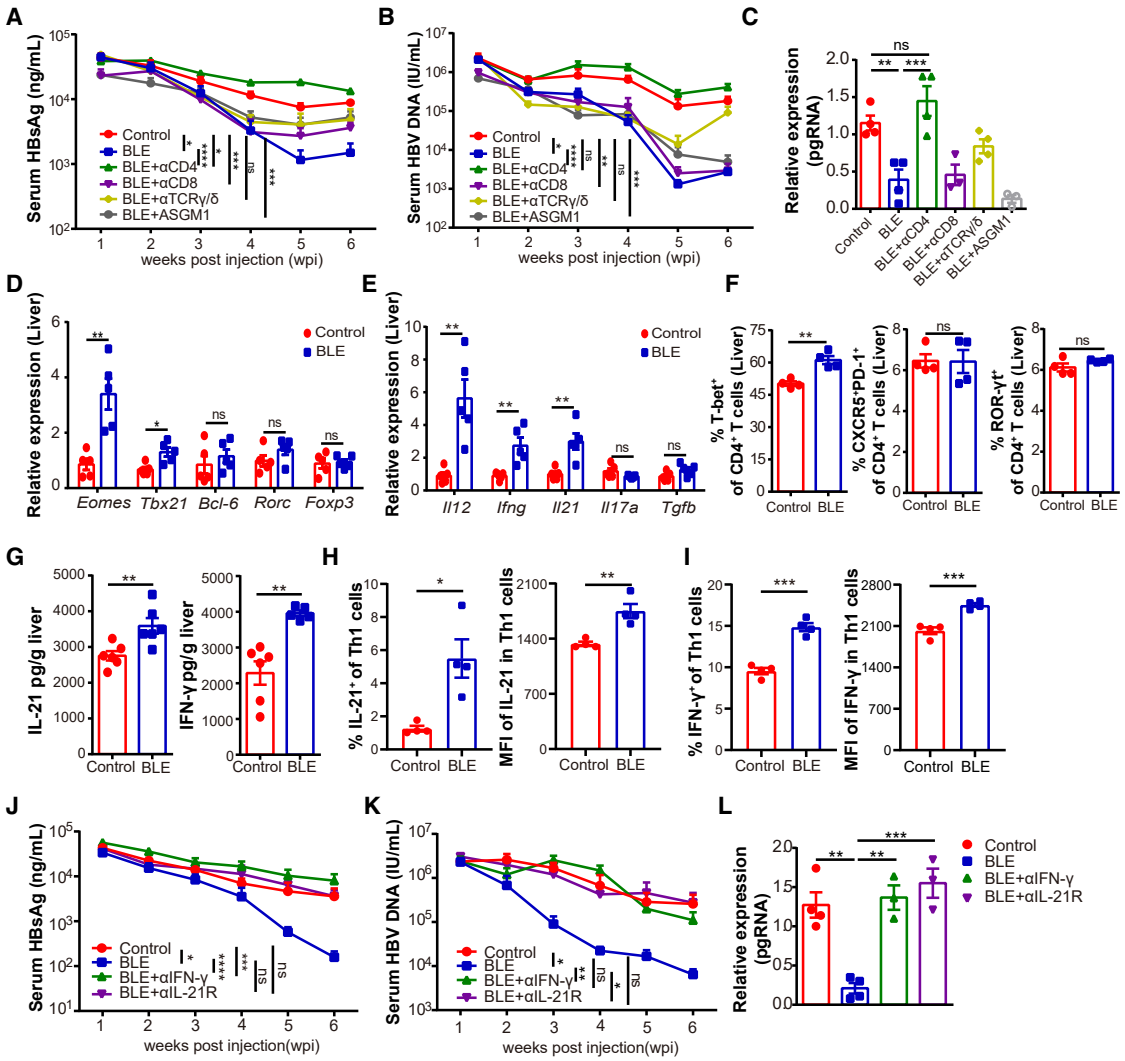

Figure 3. Depletion of CD4$^+$ T cells and inactivation of IL-21 or IFN-γ abrogated the probiotics-initiated anti-HBV effects

(A–C) Mice were treated i.p. with 100 mg neutralization antibody or isotype every 3 days from 0 to 6 wpi (control, $n = 7$; BLE, $n = 7$; BLE+αCD4, $n = 9$; BLE+αCD8, $n = 5$; BLE+αTCRγ/δ, $n = 7$; BLE+AsGM1, $n = 5$). Serum levels of HBsAg (A), HBV DNA (B), and liver pgRNA (C) were detected by ELISA and qPCR. HBV-carrier mice were treated with BLE or control PBS.

(D and E) RT-qPCR analysis of transcription factors (D) and cytokines (E) in liver tissues.

(F) FCM analysis of percentages of hepatic T-bet$^+$ Th1 cells, PD-1$^+$CXCR5$^+$ Tfh cells, and RORγt$^+$ Th17 cells among CD4$^+$ T cells.

(G) IL-21 and IFN-γ in liver homogenates were analyzed by ELISA.

(H and I) Percentages and MFI of IL-21 (H) and IFN-γ (I) in hepatic T-bet$^+$Th1 cells.

(J–L) Antibody-mediated blockade of IL-21R and IFN-γ abolished the effect of probiotics-induced HBV clearance. Mice were treated i.p. with 100 mg neutralization antibody (anti-IL-21R and anti-IFN-γ) or isotype every 3 days from 0 to 6 wpi (control, $n = 7$; BLE, $n = 7$; BLE+αIL-21R, $n = 4$; BLE+αIFN-γ, $n = 7$). Serum levels of HBsAg (J), HBV DNA (K), and liver pgRNA (L) were detected by ELISA and qPCR.

Data were expressed as mean ± SEM. The statistical tests were performed using two-way ANOVA with Dunnett's multiple comparison test (A, B, J, and K) or t test. ns, no significance; *0.01 < p value < 0.05; **0.001 < p value < 0.01; ***0.0001 < p value < 0.001; ****p value < 0.0001.

IFN-γ and IL-21 produced by CD4$^+$ T cells are indispensable for BLE-induced HBV clearance

To further evaluate the role of individual immune subsets in probiotics-mediated HBV clearance, AsGM1 and neutralized antibodies against CD4, CD8, and TCRγ/δ were used in probiotics-treated HBV-carrier mice. As shown in Figures 3A–3C, depletion of CD8$^+$ T cells, γδT cells, or natural killer (NK) cells partially restored the reduced serum levels of HBsAg in BLE-treated mice. Notably, depletion of CD4$^+$ T cells almost completely abolished BLE-induced HBV clearance, suggesting that BLE promotes HBV clearance in a CD4$^+$ T cell-dependent manner. In line with the critical role of CD4$^+$ T cells, probiotics treatment led to augmentation of CD44$^+$CD62L$^-$ effector CD4$^+$ T cells and CD44$^+$CD62L$^+$ central memory CD4$^+$ T cells in the spleen and liver (Figure S2A).

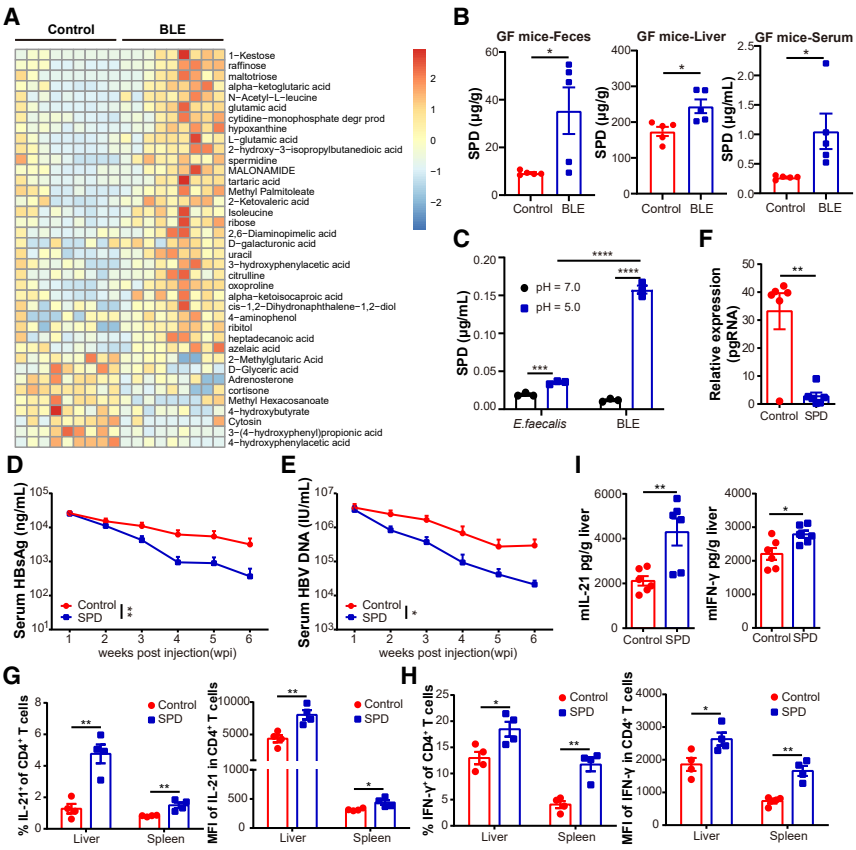

Figure 4. BLE-derived spermidine promoted HBV clearance

(A) Untargeted metabolomic analysis of feces from control and BLE mice by gas chromatograph system coupled with a Pegasus HT time-of-flight mass spectrometer (GC-TOF-MS). Heatmap of differentially expressed metabolites in mice fed with BLE were shown (control, $n = 9$; BLE, $n = 9$).

(B) Targeted metabolomics analysis of SPD in feces, peripheral serum, and livers from GF mice.

(C) Extracellular SPD concentrations in cultures of separate *E. faecalis* and mixed BLE in gifu anaerobe medium (GAM) medium supplemented with 2 mM arginine under different pH values.

(D–F) HBV-carrier mice were fed with drinking water (control, $n = 8$) or 3 mM SPD-containing water (SPD, $n = 8$). Levels of serum HBsAg (D), HBV DNA (E), and liver pgRNA (F) were detected by ELISA or qPCR.

(G and H) FCM analysis of percentages and MFI of hepatic/splenic IL-21$^+$CD4$^+$ T cells (G) and IFN-γ$^+$CD4$^+$ T cells (H).

(I) IL-21 and IFN-γ in liver homogenates were analyzed by ELISA.

Data were expressed as mean ± SEM. The statistical tests were performed using t test and two-way ANOVA (D and E). *0.01 < p value < 0.05; **0.001 < p value < 0.01; ****p value < 0.0001.

Growing evidence has demonstrated the involvement of different CD4$^+$ T subsets in anti-HBV immunity.[28,29] To gain deeper insight into the role of CD4$^+$ T subsets in BLE-mediated HBV clearance, we assessed hepatic mRNA expression of signature transcription factors and cytokines of Th1, Th17, follicular helper T (Tfh), and regulatory T (Treg) cells. Quantitative reverse-transcription PCR (RT-qPCR) revealed a significant increase in the expression of *Eomes*, *Tbx21*, *Il-21*, and *Il12*, while expression of *Ifng* but not *Bcl-6*, *Rorc*, *Foxp3*, *Il17-a*, and *Tgfb* showed no significant change in BLE mice (Figures 3D and 3E). Consistently, FCM showed a significant increase of T-box expressed in T cell (T-bet)$^+$ Th1 cells, but not CXCR5$^+$PD-1$^+$ Tfh cells and ROR-γt$^+$ Th17 cells, in the livers from BLE-treated mice (Figure 3F). In accordance, BLE treatment led to the accumulation of IL-21$^+$CD4$^+$ T cells and IFN-γ$^+$CD4$^+$ T cells in the liver and spleen (Figures S2B–S2E). In addition, ELISA revealed higher levels of IL-21 and IFN-γ in liver homogenate in BLE mice (Figure 3G). Tfh cells have been known as one of the main sources of IL-21 and IFN-γ.[30] Further analysis revealed that the expression of IL-21 and IFN-γ significantly increased in Th1 cells, but not in Tfh cells, after BLE treatment (Figures 3H, 3I, S2F, and S2G). It has been reported that IL-21 signaling enhances cytotoxicity and IFN-γ production in NK and CD8$^+$ T cells.[31] Consistently, BLE treatment increased the production of IFN-γ in splenic CD8$^+$ T cells (Figures S2H and S2I), indicating the potential contribution of CD8$^+$ T cells to BLE-induced HBV clearance. In addition, BLE treatment also led to the augmentation of hepatic and splenic IFN-γ$^+$CD4$^+$ T cells in GF mice (Figures S2J and S2K).

Considering the critical role of IFN-γ and IL-21 in determining HBV persistence,[16,32] we therefore determined whether the clearance of HBV in probiotics-treated mice is mediated by the up-regulation of IL-21 or IFN-γ. As shown in Figures 3J–3L, the treatment of neutralized antibodies against either IL-21R or IFN-γ completely abolished the anti-HBV effect mediated by probiotics treatment. In summary, these results illustrate that the probiotics administration enables the host to clear HBV by enhancing the production of IL-21 and IFN-γ in CD4$^+$ Th1 cells.

SPD produced by BLE promotes HBV clearance

The microbiota-derived metabolites serve as important signals contributing to gut homeostasis and host immunity. We then investigated whether probiotics affect the microbial metabolism of the host. Phylogenetic investigation of communities by reconstruction of unobserved states (PICRUSt) analysis of 16S rRNA sequencing data indicated the enrichment of metabolism-related pathways in BLE-treated mice (Figure S3A; Table S1). In accordance, the gas chromatograph coupled with a Pegasus HT time-of-flight mass spectrometer (GC-TOF-MS) detected the alteration of metabolites in feces from BLE-treated mice. Pathway enrichment analysis using MetaboAnalyst 5.0 (https://www.metaboanalyst.ca) showed that multiple metabolic pathways were significantly enriched in BLE mice, and 15 of them were consistent with the results of PICRUSt analysis (Figures S3A and S3B; the same pathways marked in red). Totally, untargeted metabolomic analysis showed that 38

metabolites were significantly different between control and BLE mice (Figures 4A and S3C). Among them, oligosaccharides (1-kestose, raffinose, maltotriose), amino acids (N-Acetyl-L-leucine, glutamic acid), and polyamine (SPD) were the most varied enriched metabolites. Recently, studies showed that SPD modulates $CD4^+$ T cell differentiation and enhances vaccine-induced T cell function.[33,34] Further targeted metabolomics analysis of polyamines (including SPD, spermine, and putrescine) demonstrated that SPD and putrescine rather than spermine were accumulated in the livers of BLE mice, and the concentration of SPD was higher than that of putrescine (Figure S3D). More importantly, the concentration of SPD was accumulated in the feces, peripheral serum, and livers from BLE-treated GF mice (Figure 4B). These results indicate that BLE-produced SPD may translocate from the intestine to the liver through the blood circulation.

It has been recently reported that bioactive polyamine can be produced by a hybrid system involving the collaboration of two bacterial groups and triggered by environmental acidification. In this system, *E. faecalis*, one of the three probiotic strains in BLE, functions as agmatine deiminase system to promote the production of polyamine by the collaboration of bacteria that have an acid resistance system composed of arginine decarboxylase (AdiA) and arginine-agmatine antiporter (AdiC), such as *E. coli* and *B. longum.*[35] We thus hypothesized whether the augmented SPD in the liver of BLE mice was attributed to the accumulation of BLE. To address this, we first used traditional bacterial culture methods to obtain culture supernatant and detect SPD concentration. We found that cultured BLE produced significantly higher level of SPD in the arginine-containing medium at pH 5.0 than at pH 7.0 (Figure 4C). Moreover, administration of BLE produced markedly higher levels of SPD in the feces, liver tissues, and serum of antibiotics (ABX)-treated mice, while single *E. faecalis* was not effective to produce SPD both *in vitro* and *in vivo* (Figures 4C and S4A–S4C). Accordingly, in comparison to control and single *E. faecalis*-administrated mice, BLE administration significantly decreased the serum levels of HBsAg, HBV DNA, and hepatic pgRNA (Figures S4D–S4F). Similar results were observed in FCM analysis of IFN-γ^+CD4^+ T cells in mice livers (Figure S4G). Thus, BLE effectively produces SPD and enhances anti-HBV immunity, with *E. faecalis* being able to produce SPD with the cooperation of *B. longum* and *L. acidophilus*.

We then further investigated the role of SPD in HBV clearance. Expectedly, SPD administration alone significantly decreased the levels of serum HBsAg, HBV DNA, and hepatic pgRNA in HBV-carrier mice (Figures 4D–4F). In addition, SPD administration did not cause liver injury (Figures S5A and S5B). Taken together, these results imply that BLE-derived SPD accumulated from the gut to the liver by peripheral circulation, which contributes to HBV clearance in mice.

SPD improves intestinal homeostasis and enhances Th1 cell immunity through autophagy

To further explore the mechanism underlying SPD-mediated HBV clearance, gut integrity and T cell immunity were evaluated. As shown in Figures S5C–S5E, mice fed with SPD displayed a notable elevation in intestinal *Claudin1* expression, accompanied by a clear reduction in serum levels of FITC-dextran and iFABP. This finding aligns with a previous report showing that SPD regulates the intestinal epithelial barrier function.[36] Additionally, SPD feeding led to a great increase in the expression of intestinal IL-17A, IL-21, and IL-22 and the rise in the percentages and MFI of intestinal $IL\text{-}17A^+CD4^+$ T cells, $IL\text{-}21^+CD4^+$ T cells, and $IL\text{-}22^+CD4^+$ T cells (Figures S5F–S5J). Furthermore, consistent with the results in BLE-treated mice, we detected a marked increase in the frequency of $IL\text{-}21^+CD4^+$ T cells and IFN-γ^+CD4^+ T cells in livers and spleens from SPD-treated mice (Figures 4G and 4H). ELISA confirmed the significantly increased levels of IL-21 and IFN-γ in liver homogenate from SPD mice (Figure 4I), suggesting that SPD enhances $CD4^+$ T cell immunity in HBV-carrier mice.

It has been shown that SPD, a natural autophagy-promoting polyamine, exerts multiple functions, including extending lifespan and immune cell activation, in an autophagy-dependent manner.[37] Therefore, we investigated whether SPD enhances $CD4^+$ T cell function via regulating the autophagy pathway. To address this issue, *in vitro* splenic cells isolated from OT-II mice were stimulated with ovabumin ($OVA_{323\text{-}339}$) peptide with or without SPD. FCM confirmed that SPD enhanced the production of IFN-γ in OVA-stimulated OT-II $CD4^+$ T cells in a dose-dependent manner (Figure 5A). Concurrently, SPD dose-dependently promoted the accumulation of autophagosomes in OT-II $CD4^+$ T cells (Figure 5B), while the autophagy inhibitor 3-methyladenine (3-MA, 1 mM) further enhanced the SPD-induced accumulation of autophagosomes (SPD+3-MA, Figure 5C), suggesting the activation of autophagy in SPD-treated $CD4^+$ T cells. Notably, 3-MA markedly decreased the SPD-induced augmentation of IFN-γ in $CD4^+$ T cells (Figure 5D). In line with the notion that SPD acts as the only known substrate for the hypusination of eukaryotic translation initiation factor 5A (eIF5A), which is essential for the synthesis of the autophagy transcription factor EB (TFEB),[38] treatment with GC7 (SPD+GC7), a specific inhibitor of eIF5A hypusination, decreased the accumulation of SPD-induced autophagosomes (Figure 5C) and completely damaged SPD-induced accumulation of IFN-γ in $CD4^+$ T cells (Figure 5D). Consistently, SPD induced autophagosome accumulation in hepatic $CD4^+$ T cells from HBV-carrier mice (Figure 5E). More importantly, SPD significantly promoted the accumulation of autophagosomes and IFN-γ in $CD4^+$ T cells derived from peripheral blood of HBV patients, while treatment of GC7 largely damaged this induction (Figures 5F and 5G). Taken together, these data imply that SPD enhances $CD4^+$ T cell function in an autophagy-dependent manner.

BLE accelerates the decline of serum HBsAg in human flora-associated mice and HBV patients with antiviral treatment

To address whether the probiotics would cause similar alterations in a more natural microbiome and evaluate the pre-clinical therapeutic potential of BLE and SPD in HBV clearance, we constructed the human flora-associated (HFA) model by reconstituting the microbiota of GF mice with fecal samples from HBV patients. Three weeks later, the HFA mice were injected with

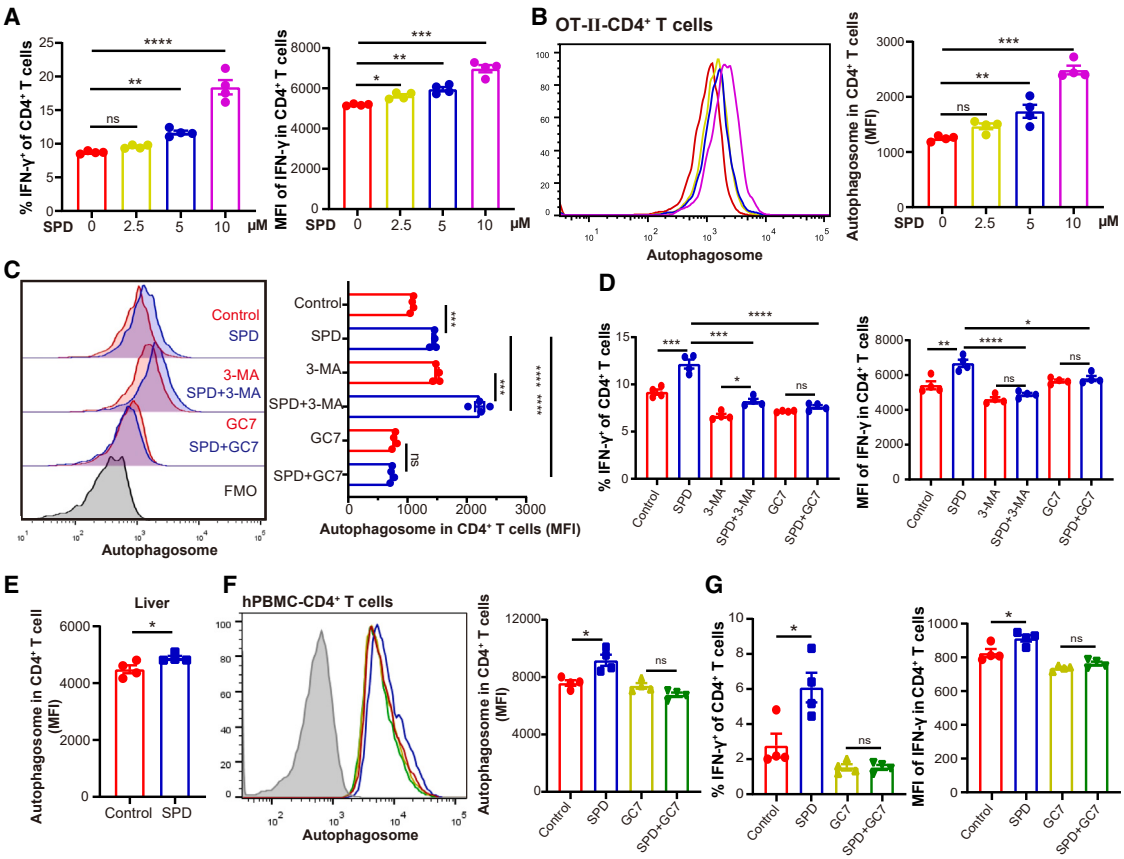

Figure 5. SPD enhanced CD4$^+$ T cell function through autophagy *in vivo* and *in vitro*

(A–D) OT-II CD4$^+$ T cells were prepared by culturing splenic mononuclear cells isolated from OT-II mice with $OVA_{323-339}$ peptide for 3 days. OT-II CD4$^+$ T cells were then treated for 24 h with increasing concentrations of SPD (A and B). 3-MA (1 mM) and GC7 (10 μM) were used to inhibit autophagy (C and D). IFN-γ levels (A and D) and autophagosome levels (B and C) in CD4 $^+$ T cells were measured by FCM.

(E) Hepatic mononuclear cells were isolated from HBV mice, and levels of autophagosome in CD4 $^+$ T cells were measured by FCM.

(F and G) PBMCs isolated from HBV patients were stimulated with SPD and/or GC7 for 24 h. Autophagosome levels (F) and IFN-γ levels (G) in CD4$^+$ T cells were measured by FCM.

Data were expressed as mean ± SEM. The statistical tests were performed using t test. ns, no significance; *0.01 < *p* value < 0.05; **0.001 < *p* value < 0.01; ***0.0001 < *p* value < 0.001; ****p value < 0.0001.

AAV/HBV1.2 by HDI and treated with either BLE or SPD, PBS as control (Figure 6A). As shown in Figures 6B–6D, both BLE and SPD showed significantly higher capacity of HBV clearance in HFA mice. Compared with PBS-treated HFA mice, BLE/SPD-treated HFA mice showed remarkably decreased levels of serum HBsAg, HBV DNA, and hepatic pgRNA. Both BLE and SPD significantly promoted the accumulation of autophagosomes in hepatic CD4$^+$ T cells (Figure 6E) and enhanced the production of IFN-γ in hepatic and splenic CD4$^+$ T cells (Figures 6F and S6A). More importantly, both BLE and SPD significantly enhanced the production of IFN-γ in hepatic and splenic HBV-specific CD4$^+$ T cells, indicating the potential contribution of BLE and SPD to HBV-specific immunity (Figures 6G, S6B, and S6C).

We therefore conducted the preliminary observation for clinical effects of BLE combined with antiviral treatment in HBV patients with persistent low level of serum HBsAg (less than 2,000 IU/mL), which were usually considered as advantaged population trend for functional cure[39] (Tables S2 and S3; Figure 6H). The dynamic profiles of serum HBsAg levels before and after BLE treatment have been illustrated (Figure S7A). Compared with control patients, patients with BLE treatment for 6 months showed an obvious decline of serum HBsAg and HBeAg (Figures 6I and S7B). In detail, all 10 patients presented a declined trend of serum HBsAg level, and 3 of 10 patients even obtained the successful loss of serum HBsAg after the treatment (patients B5, B6, B7). Notably, patient B5 and B6 maintained the state of HBsAg negative for 6 months (Figure S7A). Expectedly, BLE supplement significantly promoted the accumulation of autophagosomes and IFN-γ expression in CD4$^+$ T cells from peripheral blood mononuclear cells (PBMCs) (Figures 6J and 6K). Although this study was a preliminary observation with small number of patients, these results clearly suggest the therapeutic potential of BLE toward the functional cure of HBV infection.

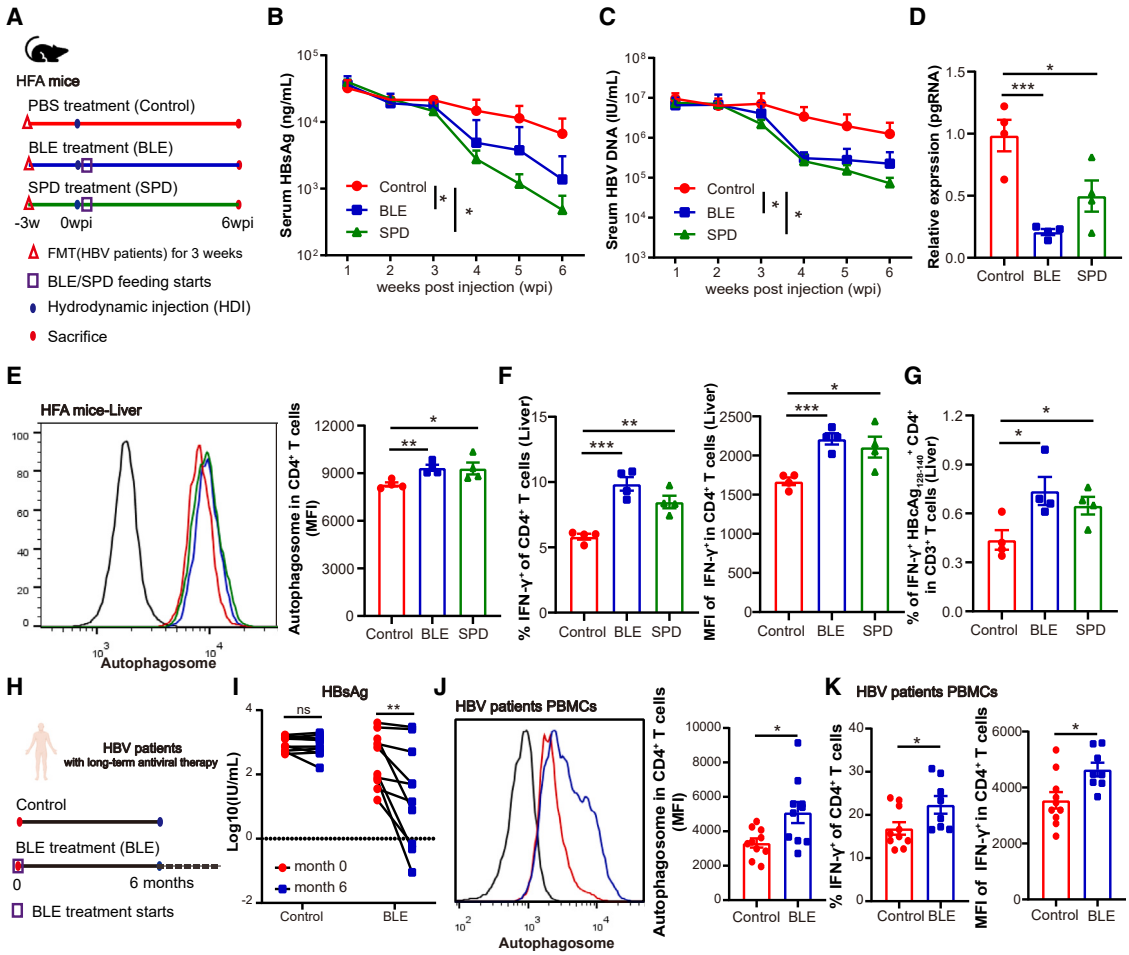

Figure 6. Probiotics accelerated HBsAg clearance in HFA mice and HBV patients

(A) Study design: male three-week-old C57BL/6J GF mice were fed with fecal microbiota from HBV patients daily for 3 weeks and then hydrodynamically injected with AAV/HBV1.2 plasmid and fed with BLE or SPD for 6 weeks (control, $n = 4$; BLE, $n = 4$; SPD, $n = 4$).

(B–D) Levels of serum HBsAg (B), HBV DNA (C), and hepatic pgRNA (D) were detected by ELISA and qPCR.

(E and F) Levels of autophagosome (E) and IFN-γ (F) in $CD4^+$ T cells were measured by FCM.

(G) MHC II-$HBcAg_{128-140}$-Tetramer was used to evaluate HBV-specific $CD4^+$ T cells. Percentages of IFN-γ in hepatic HBV-specific $CD4^+$ T cells were measured by FCM.

(H) A total of 20 eligible patients who remained persistently positive for HBsAg following >6 months of ongoing nucleos(t)ide analogs- or PegIFNα2b-based antiviral therapy were enrolled; among them, 10 patients received BLE therapy (control, $n = 10$; BLE, $n = 10$).

(I) HBsAg levels in each patient before and after BLE treatment were analyzed and compared with HBV patients without BLE treatment.

(J and K) Levels of autophagosome (J) and IFN-γ (K) in $CD4^+$ T cells from PBMCs were measured by FCM.

Data were expressed as mean ± SEM. The statistical tests were performed using two-way ANOVA with Dunnett's multiple comparison test (B and C) or t test. *0.01 < p value < 0.05; **0.001 < p value < 0.01; *** 0.0001 < p value < 0.001.

SPD synergically enhances the anti-HBV effect of entecavir in mice

Based on the aforementioned data proving the role of SPD in T cell activation and HBV clearance, we next determined whether co-administration of SPD could enhance the therapeutic effect of entecavir (ETV), the most widely used medication that efficiently inhibits HBV DNA replication but not HBsAg production.[40] As shown in Figures 7A–7D, compared to ETV monotherapy, which only suppressed HBV DNA level and showed minimal effects on HBsAg and pgRNA, the combination therapy (ETV+SPD) group demonstrated a more pronounced reduction in HBsAg and pgRNA levels, while displaying comparable inhibitory effects on HBV DNA. In accordance with the promotion of Th1 immunity in BLE-treated mice, RT-qPCR detected significantly increased expression of *Il21*, *Ifng*, *Il12*, *Tbx21*, and *Eomes* in mice with co-administration of ETV with SPD but not in mice with ETV monotherapy (Figure 7E). Furthermore, compared with ETV monotherapy, combination therapy significantly increased the production of IFN-γ in splenic and hepatic $CD4^+$ T cells (Figures 7F and 7G). Taken together, these data demonstrate that SPD greatly enhances the anti-HBV therapeutic effect of ETV by promoting antiviral immunity and suggest the therapeutic potential of SPD toward the functional cure of HBV infection.

CellPress
OPEN ACCESS

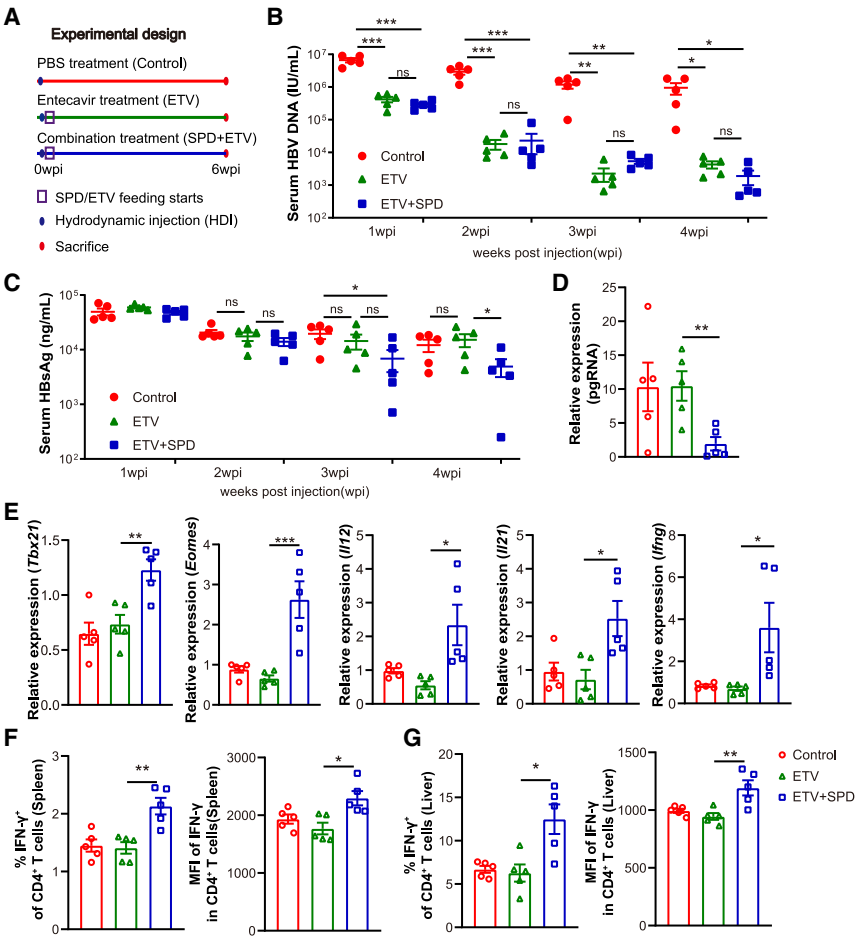

Figure 7. Combination of SPD promoted the HBV inhibition in HBV-carrier mice

(A) Male five-week-old HBV-carrier mice were administered with entecavir (ETV) or co-administered with 3 mM SPD water (ETV+SPD) combined with ETV (control, n = 5; SPD, n = 5; ETV, n = 5; ETV+SPD, n = 5).

(B–D) Levels of serum HBsAg (B), HBV DNA (C), and liver pgRNA (D) were detected by ELISA or qPCR.

(E) RT-qPCR analysis of transcription factors and cytokines in liver tissues.

(F and G) FCM analysis of percentages and MFI of splenic (F) and hepatic (G) IFN-γ^+CD4$^+$ T cells.

Data were expressed as mean ± SEM. The statistical tests were performed using t test. ns, no significance; *0.01 < p value < 0.05; **0.001 < p value < 0.01; *** 0.0001 < p value < 0.001.

DISCUSSION

Functional cure of HBV infection is considered an achievable therapeutic goal, given that it is almost universally observed after adult infection. However, the current anti-HBV drugs, namely nucleos(t)ide analogs as well as peginterferon-α (PegIFNα), cured fewer than 1% in the natural history of chronic HBV infection.[41] The high burden of viral antigens that promote T cell exhaustion with T cell dysfunction is the key barrier to functional cure.[8] In this study, we demonstrate the critical role of probiotics in enhancing CD4$^+$ T cell function and promoting the clearance of HBV. Furthermore, probiotics showed the potential to accelerate the decline of serum HBsAg levels in HBV patients with common anti-HBV drugs. Probiotics are widely used as food supplement to assist in the treatment of many health conditions,[21] and no liver injury was detected in mice treated with BLE in our studies. Our data here provide a safe and effective combination intervention strategy for chronic HBV infection.

Scientific evidence supports the important roles of probiotics in alleviating the symptoms of several digestive system diseases.[21] A large number of studies also have demonstrated the disturbed gut microbiota in HBV patients.[42] In this study, using 16S rRNA sequencing, we showed that probiotics administration alters microbiome compositions and enriches commensal diversity in HBV-carrier mice. Further, qPCR analysis using bacterium-specific primers showed the accumulation of BLE in probiotics-treated mice. Then, FMT experiments and GF mice were used to verify that accumulation of BLE contributes to HBV clearance. Therapeutic strategies to cure persistent HBV infection almost invariably include approaches to enhance antiviral T cell immunity.[43] Our data suggest that BLE-induced HBV clearance is achieved by provoking CD4$^+$ T cell function. Depletion of CD4$^+$ T cells, as well as blocking IL-21 and IFN-γ, the well-known effector molecules of CD4$^+$ Th1 cells, almost abolished BLE-initiated HBV clearance. Further expression analysis of signature transcription factors of different CD4$^+$ T cell subsets demonstrated the augmented expression of *Tbx21* and *Eomes* but not *Bcl-6*, *Rorc*, and *Foxp3* in probiotics-treated mice, suggesting the involvement of Th1 cells in probiotics-mediated HBV clearance. Although T-bet was also involved in Tfh cell development and germinal center generation, and expression of IL-21 and IFN-γ is detected in Tfh cells,[44] FCM analysis showed no alteration in either IL-21$^+$ Tfh or IFN-γ$^+$ Tfh cells in BLE-treated mice. Meanwhile, BLE treatment did not influence the production of HBsAb (Table S4). These results suggest that Th1 but not Tfh cells were the main effector cells contributing to BLE-induced HBV clearance.

Another finding of our study is that we have demonstrated that SPD is the key metabolite responsible for HBV clearance and is produced by BLE. Firstly, PICRUSt analysis of 16S rRNA sequencing data and untargeted metabolomic analysis showed that the metabolism-related pathways, especially amino acid metabolism, were significantly enriched in mice with probiotics treatment. In particular, D-glutamine and D-glutamate metabolism and glutamic acid were the most abundant altered amino acid-related pathways and metabolites. It has been reported that glutamine metabolism promotes effector T cell generation and function,[45] and glutamic acid is a highly effective regulator in initiating T cell-mediated immune

responses.[46] Moreover, beta-alanine metabolism, arginine and proline metabolism, and glutathione metabolism pathway contain the common metabolite SPD, which also enhanced the IFN-γ production of $CD8^+$ T cells.[33] Secondly, targeted metabolomics analysis identified the enrichment of SPD in feces and livers from BLE-treated SPF mice. Moreover, single administration of SPD led to similar effects as probiotics in inhibiting HBV replication as well as improving intestinal homeostasis and Th1 cell function. Importantly, BLE supplementation increased SPD content in feces, peripheral serum, and livers and promoted HBV clearance in GF mice. Previous studies reported that SPD can be produced by many other microorganisms, such as *Prevotellaceae*, *Clostridiaceae*, and *Ruminococcaceae*.[47] It needs to be further investigated whether BLE-induced alteration of other SPD-producing strains also participates in HBV clearance in SPF mice.

Accumulated data demonstrated the effect of SPD on immunity, while its immunomodulatory effect was context dependent.[34,37,38] SPD shifts Th17 cell polarization toward Tregs, while it did not affect the production of IFN-γ of naive $CD4^+$ T cells under Th1-polarizing conditions.[34] Matsumoto et al. reported increased IFN-γ and augmented fecal polyamine in probiotics-treated patients with autoimmunity.[48] Our studies confirmed that SPD administration enhanced $CD4^+$ T cell function and promoted HBV clearance *in vivo*. SPD, a natural autophagy-promoting polyamine, exerts multiple functions, mainly through autophagy. It acts as the only known substrate for the hypusination eIF5A, which is essential for the synthesis of the autophagy transcription factor TFEB.[38] *In vitro* studies showed that both autophagy inhibitor 3-MA and eIF5A-hypusine inhibitor GC7 significantly decrease SPD-induced IFN-γ accumulation in $CD4^+$ T cells. Therefore, our work revealed that the SPD-autophagy pathway enhanced IFN-γ^+CD4^+ T cell immunity. However, other metabolites, especially oligosaccharides (1-kestose, raffinose, maltotriose), which are used as prebiotics to regulate the immune system,[49,50] were also up-regulated after probiotics treatment. Therefore, more work is required to determine the key metabolism-related pathways and master metabolites contributing to HBV clearance.

The seroclearance or seroconversion of HBsAg has been identified as the key marker for HBV cure in clinics. However, the spontaneous conversion rate of HBsAg is as low as less than 1% in the natural population[7] and as high as no more than 30% even in patients with HBsAg levels <1,000 IU/mL.[51] Notably, our preliminary observational study reported that probiotics accelerate the decline of serum HBsAg levels in patients receiving anti-HBV drugs. Importantly, 3 of 10 patients obtained the successful loss of serum HBsAg after the treatment with PegIFNα2b and tenofovir in combination with probiotics. Although the sample size is small, the exciting data still showed the great potential of probiotics in the loss of HBsAg. A combination of probiotics or SPD and antiviral treatment might be the potential therapeutic strategy for HBV functional cure.

In conclusion, SPD derived from BLE effectively promotes HBV clearance, which is likely to associate with more effective IFN-γ^+CD4^+ Th1 cells. Our study has offered valuable insight into the immune mechanism of microbiota-mediated HBV clearance. Furthermore, it provides possible cues to use probiotics and SPD combination therapy with anti-HBV drugs in the clinical treatment of chronic HBV infection.

Limitations of the study

Our study has some limitations. We used mice with hydrodynamic injection of AAV/HBV1.2 as the mouse model to perform HBV clearance studies. Although this is a commonly used HBV model, hydrodynamic injection induces the release of damage-associated molecular patterns upon hepatocellular death. This process is in sharp contrast to the stealthy nature of HBV, which typically evades from the innate immune detection machinery during natural infections.[52] Besides, although the exciting data have been obtained in human beings, perspective and randomized controlled trial is required to confirm the therapeutic potential of BLE as well as the identified metabolite in the context of HBV inhibition. Moreover, although both BLE and SPD contributed to the function of HBV-specific $CD4^+$ T cells, whether they could suppress other pathogens by modulating host immunity needs to be further verified.

RESOURCE AVAILABILITY

Lead contact

Further information and requests for resources and reagents should be directed to and will be fulfilled by the lead contact, Chunhong Ma (machunhong@sdu.edu.cn).

Materials availability

All unique/stable reagents generated in this study are available from the lead contact upon request and upon completion of Materials Transfer Agreement.

Data and code availability

- 16S rRNA sequencing data in this study have been deposited in the National Center for Biotechnology Information (NCBI) database under BioProject accession number SRA: PRJNA700493. Metabolomics data in this study have been deposited in the National Metabolomics Data Repository (NMDR) under Study ID ST003536.
- This paper does not report original code.
- Any additional information required to reanalyze the data reported in this paper is available from the lead contact upon request.

ACKNOWLEDGMENTS

We would like to thank the participants who have made this research possible. We thank the Translational Medicine Core Facility of Shandong University for the consultation and instrument availability that supported this work. This work was supported by grants from the National Key R&D Program of China (2022YFC2303600, 2022YFC2304500), the National Natural Science Foundation of China (81830017, 82321002, 82171805, 82270631, 82471870, and 32200742), National Center of Technology Innovation for Biopharmaceuticals (NCTIB2023XB02006), Cutting Edge Development Fund of Advanced Medical Research Institute (GYY2023QY01), Taishan Scholarship (tstp20231212), and Major Basic Research Project of Shandong Natural Science Foundation (no. ZR2020ZD12).

AUTHOR CONTRIBUTIONS

Conceptualization, C.M.; methodology, T.W., Y.F., C.L., X.L., and C.M.; investigation, T.W., Y.F., S.T., Z.W., X.G., M.L., X.Y., Q.L., X.S., and L.X.; writing – original draft, T.W.; writing – review and editing, T.W., Y.F., S.T., Z.W., X.G., M.L., X.Y., Q.L., X.S., L.X., L.L., S.L., L.G., X.L., C.L., and C.M.; supervision,

Y.F., C.L., L.L., S.L., L.G., X.L., and C.M.; funding acquisition, Y.F., X.L., C.L., S.T., and C.M.

DECLARATION OF INTERESTS

C.M., T.W., L.G., X.L., C.L., Z.W., S.T., X.S., Q.L., X.Y., and M.L. are inventors on the China patent (ZL202010499490X) "Application of spermidine in the preparation of anti-hepatitis B virus drugs" that has claims directed to spermidine application in anti-HBV immunity.

STAR★METHODS

Detailed methods are provided in the online version of this paper and include the following:

- KEY RESOURCES TABLE
- EXPERIMENTAL MODEL AND STUDY PARTICIPANT DETAILS
  - Mice
  - Plasmids
  - HBV mouse model
  - Probiotics, spermidine and entecavir administration
  - Fecal microbiota transplantation
  - Patients
- METHOD DETAILS
  - FITC-dextran administration and *In vivo* neutralization
  - Enzyme-linked immunosorbent assays (ELISA)
  - Quantitative real-time PCR
  - Quantitation of HBV replication
  - Northern blot
  - Cell isolation and culture
  - Flow cytometry
  - MHC class II tetramer
  - 16S rRNA sequencing
  - Metabolomics
  - Evaluation of SPD in culture of BLE or *Enterococcus faecalis*
  - Statistical analysis

SUPPLEMENTAL INFORMATION

Supplemental information can be found online at https://doi.org/10.1016/j.xcrm.2024.101822.

Received: March 17, 2024
Revised: July 30, 2024
Accepted: October 17, 2024
Published: November 12, 2024

REFERENCES

1. Seto, W.K., Lo, Y.R., Pawlotsky, J.M., and Yuen, M.F. (2018). Chronic hepatitis B virus infection. Lancet *392*, 2313–2324. https://doi.org/10.1016/s0140-6736(18)31865-8.
2. Gehring, A.J., and Protzer, U. (2019). Targeting Innate and Adaptive Immune Responses to Cure Chronic HBV Infection. Gastroenterology *156*, 325–337. https://doi.org/10.1053/j.gastro.2018.10.032.
3. Nayagam, S., Thursz, M., Sicuri, E., Conteh, L., Wiktor, S., Low-Beer, D., and Hallett, T.B. (2016). Requirements for global elimination of hepatitis B: a modelling study. Lancet Infect. Dis. *16*, 1399–1408. https://doi.org/10.1016/s1473-3099(16)30204-3.
4. Naggie, S., and Lok, A.S. (2021). New Therapeutics for Hepatitis B: The Road to Cure. Annu. Rev. Med. *72*, 93–105. https://doi.org/10.1146/annurev-med-080119-103356.
5. Dolgin, E. (2022). Closing in on a cure for hepatitis B. Nature *603*, S46–S48. https://doi.org/10.1038/d41586-022-00812-1.
6. Hsu, Y.C., Huang, D.Q., and Nguyen, M.H. (2023). Global burden of hepatitis B virus: current status, missed opportunities and a call for action. Nat. Rev. Gastroenterol. Hepatol. *20*, 524–537. https://doi.org/10.1038/s41575-023-00760-9.
7. Tseng, T.C., Chiang, C., Liu, C., Liu, C.J., Su, T.H., Yang, H.C., Yang, W.T., Liu, C., Chen, P.J., and Kao, J.H. (2023). Low Hepatitis B Core-Related Antigen Levels Correlate Higher Spontaneous Seroclearance of Hepatitis B Surface Antigen in Chronic Hepatitis B Patients With High Hepatitis B Surface Antigen Levels. Gastroenterology *164*, 669–679.e6. https://doi.org/10.1053/j.gastro.2023.01.005.
8. Laupèze, B., Vassilev, V., and Badur, S. (2023). A role for immune modulation in achieving functional cure for chronic hepatitis B among current changes in the landscape of new treatments. Expet Rev. Gastroenterol. Hepatol. *17*, 1135–1147. https://doi.org/10.1080/17474124.2023.2268503.
9. Jacobi, F.J., Wild, K., Smits, M., Zoldan, K., Csernalabics, B., Flecken, T., Lang, J., Ehrenmann, P., Emmerich, F., Hofmann, M., et al. (2019). OX40 stimulation and PD-L1 blockade synergistically augment HBV-specific CD4 T cells in patients with HBeAg-negative infection. J. Hepatol. *70*, 1103–1113. https://doi.org/10.1016/j.jhep.2019.02.016.
10. Hoogeveen, R.C., Dijkstra, S., Bartsch, L.M., Drescher, H.K., Aneja, J., Robidoux, M.P., Cheney, J.A., Timm, J., Gehring, A., de Sousa, P.S.F., et al. (2022). Hepatitis B virus-specific CD4 T cell responses differentiate functional cure from chronic surface antigen(+) infection. J. Hepatol. *77*, 1276–1286. https://doi.org/10.1016/j.jhep.2022.05.041.
11. Wang, R., Tang, R., Li, B., Ma, X., Schnabl, B., and Tilg, H. (2021). Gut microbiome, liver immunology, and liver diseases. Cell. Mol. Immunol. *18*, 4–17. https://doi.org/10.1038/s41423-020-00592-6.
12. Shen, Y., Wu, S.D., Chen, Y., Li, X.Y., Zhu, Q., Nakayama, K., Zhang, W.Q., Weng, C.Z., Zhang, J., Wang, H.K., et al. (2023). Alterations in gut microbiome and metabolomics in chronic hepatitis B infection-associated liver disease and their impact on peripheral immune response. Gut Microb. *15*, 2155018. https://doi.org/10.1080/19490976.2022.2155018.
13. Li, Y.N., Kang, N.L., Jiang, J.J., Zhu, Y.Y., Liu, Y.R., Zeng, D.W., and Wang, F. (2022). Gut microbiota of hepatitis B virus-infected patients in the immune-tolerant and immune-active phases and their implications in metabolite changes. World J. Gastroenterol. *28*, 5188–5202. https://doi.org/10.3748/wjg.v28.i35.5188.
14. Schwabe, R.F., and Greten, T.F. (2020). Gut microbiome in HCC - Mechanisms, diagnosis and therapy. J. Hepatol. *72*, 230–238. https://doi.org/10.1016/j.jhep.2019.08.016.
15. Chou, H.H., Chien, W.H., Wu, L.L., Cheng, C.H., Chung, C.H., Horng, J.H., Ni, Y.H., Tseng, H.T., Wu, D., Lu, X., et al. (2015). Age-related immune clearance of hepatitis B virus infection requires the establishment of gut microbiota. Proc. Natl. Acad. Sci. USA *112*, 2175–2180. https://doi.org/10.1073/pnas.1424775112.
16. Publicover, J., Goodsell, A., Nishimura, S., Vilarinho, S., Wang, Z.e., Avanesyan, L., Spolski, R., Leonard, W.J., Cooper, S., and Baron, J.L. (2011). IL-21 is pivotal in determining age-dependent effectiveness of immune responses in a mouse model of human hepatitis B. J. Clin. Invest. *121*, 1154–1162. https://doi.org/10.1172/jci44198.
17. Ren, Y.D., Ye, Z.S., Yang, L.Z., Jin, L.X., Wei, W.J., Deng, Y.Y., Chen, X.X., Xiao, C.X., Yu, X.F., Xu, H.Z., et al. (2017). Fecal microbiota transplantation induces hepatitis B virus e-antigen (HBeAg) clearance in patients with positive HBeAg after long-term antiviral therapy. Hepatology *65*, 1765–1768. https://doi.org/10.1002/hep.29008.
18. Rooks, M.G., and Garrett, W.S. (2016). Gut microbiota, metabolites and host immunity. Nat. Rev. Immunol. *16*, 341–352. https://doi.org/10.1038/nri.2016.42.
19. Martínez-López, M., Iborra, S., Conde-Garrosa, R., Mastrangelo, A., Danne, C., Mann, E., Reid, D., Gaboriau-Routhiau, V., Chaparro, M., Lorenzo, M., et al. (2019). Microbiota Sensing by Mincle-Syk Axis in Dendritic Cells Regulates Interleukin-17 and -22 Production and Promotes Intestinal Barrier Integrity. Immunity *50*, 446–461.e9. https://doi.org/10.1016/j.immuni.2018.12.020.

20. Vendrik, K.E.W., Terveer, E.M., Kuijper, E.J., Nooij, S., Boeije-Koppenol, E., Sanders, I.M.J.G., van Lingen, E., Verspaget, H.W., Berssenbrugge, E.K.L., Keller, J.J., et al. (2021). Periodic screening of donor faeces with a quarantine period to prevent transmission of multidrug-resistant organisms during faecal microbiota transplantation: a retrospective cohort study. Lancet Infect. Dis. *21*, 711–721. https://doi.org/10.1016/s1473-3099(20)30473-4.

21. Sanders, M.E., Merenstein, D.J., Reid, G., Gibson, G.R., and Rastall, R.A. (2019). Probiotics and prebiotics in intestinal health and disease: from biology to the clinic. Nat. Rev. Gastroenterol. Hepatol. *16*, 605–616. https://doi.org/10.1038/s41575-019-0173-3.

22. Huang, L.R., Wu, H.L., Chen, P.J., and Chen, D.S. (2006). An immunocompetent mouse model for the tolerance of human chronic hepatitis B virus infection. Proc. Natl. Acad. Sci. USA *103*, 17862–17867. https://doi.org/10.1073/pnas.0608578103.

23. Vétizou, M., Pitt, J.M., Daillère, R., Lepage, P., Waldschmitt, N., Flament, C., Rusakiewicz, S., Routy, B., Roberti, M.P., Duong, C.P.M., et al. (2015). Anticancer immunotherapy by CTLA-4 blockade relies on the gut microbiota. Science *350*, 1079–1084. https://doi.org/10.1126/science.aad1329.

24. Gopalakrishnan, V., Spencer, C.N., Nezi, L., Reuben, A., Andrews, M.C., Karpinets, T.V., Prieto, P.A., Vicente, D., Hoffman, K., Wei, S.C., et al. (2018). Gut microbiome modulates response to anti-PD-1 immunotherapy in melanoma patients. Science *359*, 97–103. https://doi.org/10.1126/science.aan4236.

25. Katayama, Y., Yamada, T., Shimamoto, T., Iwasaku, M., Kaneko, Y., Uchino, J., and Takayama, K. (2019). The role of the gut microbiome on the efficacy of immune checkpoint inhibitors in Japanese responder patients with advanced non-small cell lung cancer. Transl. Lung Cancer Res. *8*, 847–853. https://doi.org/10.21037/tlcr.2019.10.23.

26. Chopyk, D.M., and Grakoui, A. (2020). Contribution of the Intestinal Microbiome and Gut Barrier to Hepatic Disorders. Gastroenterology *159*, 849–863. https://doi.org/10.1053/j.gastro.2020.04.077.

27. Timmermans, K., Sir, Ö., Kox, M., Vaneker, M., de Jong, C., Gerretsen, J., Edwards, M., Scheffer, G.J., and Pickkers, P. (2015). Circulating iFABP Levels as a marker of intestinal damage in trauma patients. Shock *43*, 117–120. https://doi.org/10.1097/shk.0000000000000284.

28. Boettler, T., Choi, Y.S., Salek-Ardakani, S., Cheng, Y., Moeckel, F., Croft, M., Crotty, S., and von Herrath, M. (2013). Exogenous OX40 stimulation during lymphocytic choriomeningitis virus infection impairs follicular Th cell differentiation and diverts CD4 T cells into the effector lineage by upregulating Blimp-1. J. Immunol. *191*, 5026–5035. https://doi.org/10.4049/jimmunol.1300013.

29. Hale, J.S., Youngblood, B., Latner, D.R., Mohammed, A.U.R., Ye, L., Akondy, R.S., Wu, T., Iyer, S.S., and Ahmed, R. (2013). Distinct memory CD4+ T cells with commitment to T follicular helper- and T helper 1-cell lineages are generated after acute viral infection. Immunity *38*, 805–817. https://doi.org/10.1016/j.immuni.2013.02.020.

30. Long, D., Chen, Y., Wu, H., Zhao, M., and Lu, Q. (2019). Clinical significance and immunobiology of IL-21 in autoimmunity. J. Autoimmun. *99*, 1–14. https://doi.org/10.1016/j.jaut.2019.01.013.

31. Leonard, W.J., and Spolski, R. (2005). Interleukin-21: a modulator of lymphoid proliferation, apoptosis and differentiation. Nat. Rev. Immunol. *5*, 688–698. https://doi.org/10.1038/nri1688.

32. Wang, H., Luo, H., Wan, X., Fu, X., Mao, Q., Xiang, X., Zhou, Y., He, W., Zhang, J., Guo, Y., et al. (2020). TNF-α/IFN-γ profile of HBV-specific CD4 T cells is associated with liver damage and viral clearance in chronic HBV infection. J. Hepatol. *72*, 45–56. https://doi.org/10.1016/j.jhep.2019.08.024.

33. Alsaleh, G., Panse, I., Swadling, L., Zhang, H., Richter, F.C., Meyer, A., Lord, J., Barnes, E., Klenerman, P., Green, C., and Simon, A.K. (2020). Autophagy in T cells from aged donors is maintained by spermidine and correlates with function and vaccine responses. Elife *9*, e57950. https://doi.org/10.7554/eLife.57950.

34. Carriche, G.M., Almeida, L., Stüve, P., Velasquez, L., Dhillon-LaBrooy, A., Roy, U., Lindenberg, M., Strowig, T., Plaza-Sirvent, C., Schmitz, I., et al. (2021). Regulating T-cell differentiation through the polyamine spermidine. J. Allergy Clin. Immunol. *147*, 335–348.e11. https://doi.org/10.1016/j.jaci.2020.04.037.

35. Kitada, Y., Muramatsu, K., Toju, H., Kibe, R., Benno, Y., Kurihara, S., and Matsumoto, M. (2018). Bioactive polyamine production by a novel hybrid system comprising multiple indigenous gut bacterial strategies. Sci. Adv. *4*, eaat0062. https://doi.org/10.1126/sciadv.aat0062.

36. Chen, J., Rao, J.N., Zou, T., Liu, L., Marasa, B.S., Xiao, L., Zeng, X., Turner, D.J., and Wang, J.Y. (2007). Polyamines are required for expression of Toll-like receptor 2 modulating intestinal epithelial barrier integrity. Am. J. Physiol. Gastrointest. Liver Physiol. *293*, G568–G576. https://doi.org/10.1152/ajpgi.00201.2007.

37. Madeo, F., Eisenberg, T., Pietrocola, F., and Kroemer, G. (2018). Spermidine in health and disease. Science *359*, eaan2788. https://doi.org/10.1126/science.aan2788.

38. Zhang, H., Alsaleh, G., Feltham, J., Sun, Y., Napolitano, G., Riffelmacher, T., Charles, P., Frau, L., Hublitz, P., Yu, Z., et al. (2019). Polyamines Control eIF5A Hypusination, TFEB Translation, and Autophagy to Reverse B Cell Senescence. Mol. Cell. *76*, 110–125.e9. https://doi.org/10.1016/j.molcel.2019.08.005.

39. Guan, G., Zhang, T., Ning, J., Tao, C., Gao, N., Zeng, Z., Guo, H., Chen, C.C., Yang, J., Zhang, J., et al. (2024). Higher TP53BP2 expression is associated with HBsAg loss in peginterferon-α-treated patients with chronic hepatitis B. J. Hepatol. *80*, 41–52. https://doi.org/10.1016/j.jhep.2023.09.039.

40. European Association for the Study of the Liver (2017). EASL 2017 Clinical Practice Guidelines on the management of hepatitis B virus infection. J. Hepatol. *67*, 370–398. https://doi.org/10.1016/j.jhep.2017.03.021.

41. Lim, S.G., Baumert, T.F., Boni, C., Gane, E., Levrero, M., Lok, A.S., Maini, M.K., Terrault, N.A., and Zoulim, F. (2023). The scientific basis of combination therapy for chronic hepatitis B functional cure. Nat. Rev. Gastroenterol. Hepatol. *20*, 238–253. https://doi.org/10.1038/s41575-022-00724-5.

42. Zeng, Y., Chen, S., Fu, Y., Wu, W., Chen, T., Chen, J., Yang, B., and Ou, Q. (2020). Gut microbiota dysbiosis in patients with hepatitis B virus-induced chronic liver disease covering chronic hepatitis, liver cirrhosis and hepatocellular carcinoma. J. Viral Hepat. *27*, 143–155. https://doi.org/10.1111/jvh.13216.

43. Lok, A.S., Zoulim, F., Dusheiko, G., and Ghany, M.G. (2017). Hepatitis B cure: From discovery to regulatory approval. J. Hepatol. *67*, 847–861. https://doi.org/10.1016/j.jhep.2017.05.008.

44. Weinstein, J.S., Laidlaw, B.J., Lu, Y., Wang, J.K., Schulz, V.P., Li, N., Herman, E.I., Kaech, S.M., Gallagher, P.G., and Craft, J. (2018). STAT4 and T-bet control follicular helper T cell development in viral infections. J. Exp. Med. *215*, 337–355. https://doi.org/10.1084/jem.20170457.

45. O'Neill, L.A.J., Kishton, R.J., and Rathmell, J. (2016). A guide to immunometabolism for immunologists. Nat. Rev. Immunol. *16*, 553–565. https://doi.org/10.1038/nri.2016.70.

46. Pacheco, R., Oliva, H., Martinez-Navío, J.M., Climent, N., Ciruela, F., Gatell, J.M., Gallart, T., Mallol, J., Lluis, C., and Franco, R. (2006). Glutamate released by dendritic cells as a novel modulator of T cell activation. J. Immunol. *177*, 6695–6704. https://doi.org/10.4049/jimmunol.177.10.6695.

47. Hanfrey, C.C., Pearson, B.M., Hazeldine, S., Lee, J., Gaskin, D.J., Woster, P.M., Phillips, M.A., and Michael, A.J. (2011). Alternative spermidine biosynthetic route is critical for growth of Campylobacter jejuni and is the dominant polyamine pathway in human gut microbiota. J. Biol. Chem. *286*, 43301–43312. https://doi.org/10.1074/jbc.M111.307835.

48. Matsumoto, M., Aranami, A., Ishige, A., Watanabe, K., and Benno, Y. (2007). LKM512 yogurt consumption improves the intestinal environment and induces the T-helper type 1 cytokine in adult patients with intractable

atopic dermatitis. Clin. Exp. Allergy *37*, 358–370. https://doi.org/10.1111/j.1365-2222.2007.02642.x.

49. Kim, H.J., Lee, S.H., Go, H.N., Ahn, J.R., Kim, H.J., and Hong, S.J. (2018). Effects of kestose on gut mucosal immunity in an atopic dermatitis mouse model. J. Dermatol. Sci. *89*, 27–32. https://doi.org/10.1016/j.jdermsci.2017.10.006.

50. Koga, Y., Tokunaga, S., Nagano, J., Sato, F., Konishi, K., Tochio, T., Murakami, Y., Masumoto, N., Tezuka, J.I., Sudo, N., et al. (2016). Age-associated effect of kestose on Faecalibacterium prausnitzii and symptoms in the atopic dermatitis infants. Pediatr. Res. *80*, 844–851. https://doi.org/10.1038/pr.2016.167.

51. Moini, M., and Fung, S. (2022). HBsAg Loss as a Treatment Endpoint for Chronic HBV Infection: HBV Cure. Viruses *14*, 657. https://doi.org/10.3390/v14040657.

52. Liu, Y., Maya, S., and Ploss, A. (2021). Animal Models of Hepatitis B Virus Infection-Success, Challenges, and Future Directions. Viruses *13*, 777. https://doi.org/10.3390/v13050777.

53. Yue, F., Li, W., Zou, J., Jiang, X., Xu, G., Huang, H., and Liu, L. (2017). Spermidine Prolongs Lifespan and Prevents Liver Fibrosis and Hepatocellular Carcinoma by Activating MAP1S-Mediated Autophagy. Cancer Res. *77*, 2938–2951. https://doi.org/10.1158/0008-5472.Can-16-3462.

STAR★METHODS

KEY RESOURCES TABLE

REAGENT or RESOURCE	SOURCE	IDENTIFIER
Antibodies		
Anti-mouse CD3 (145-2C11) PE	BioLegend	Cat# 100308; RRID: AB_312672
Anti-mouse CD3 (17A2) APC	BioLegend	Cat# 100236; RRID: AB_2561455
Anti-mouse CD3 (145-2C11) PE-CY7	eBioscience	Cat# 25-0031-82; RRID: AB_469572
Anti-mouse CD3 (145-2C11) APC/Fire750	BioLegend	Cat# 100362; RRID: AB_2629686
Anti-mouse CD4 (RM4-5) PerCP-Cy5.5	eBioscience	Cat# 45-0042-82; RRID: AB_1107001
Anti-mouse CD4 (GK1.5) PE-CY7	eBioscience	Cat# 25-0041-81; RRID: AB_469575
Anti-mouse CD8a (53–6.7) FITC	BioLegend	Cat# 100706; RRID: AB_312744
Anti-mouse γ/δTCR (GL3) APC	BioLegend	Cat# 118116; RRID: AB_1731824
Anti-mouse CD44 (IM7) APC	eBioscience	Cat# 17-0441-81; RRID: AB_469389
Anti-mouse CD62L (MEL-14) PE	BioLegend	Cat# 104408; RRID: AB_313094
Anti-mouse PD-1 (29F.1A12) BV421	BioLegend	Cat# 135218; RRID: AB_2561447
Anti-mouse CXCR5 (L138D7) FITC	BioLegend	Cat# 145520; RRID: AB_2562865
Anti-mouse CD25 (3C7) Alexa Flour 488	eBioscience	Cat# 53-0253-82; RRID: AB_763471
Anti-mouse CD127 (A7R34) PerCP-Cy5.5	BioLegend	Cat# 135022; RRID: AB_1937274
Anti-mouse NKp46 (29A1.4) PE-CY7	eBioscience	Cat# 25-3351-82; RRID: AB_2573442
Anti-mouse NK1.1 (PK136) PE-CY7	BD Biosciences	Cat# 552878; RRID: AB_394507
Anti-mouse Foxp3 (FJK-16s) eFlour660	eBioscience	Cat# 50-5773-82; RRID: AB_11218868
Anti-mouse T-bet (4B10) PE-CY7	eBioscience	Cat# 25-5825-82; RRID: AB_11042699
Anti-mouse T-bet (4B10) BV421	BioLegend	Cat# 644816; RRID: AB_2686976
Anti-mouse RORγt (Q31-378) BV421	BD Biosciences	Cat# 562894; RRID: AB_2687545
Anti-mouse RORγt (B2D) APC	eBioscience	Cat# 17-6981-82; RRID: AB_2573254
Anti-mouse IL-17A (TC11-18H10.1) FITC	BioLegend	Cat# 506907; RRID: AB_536009
Anti-mouse IL-21 (FFA21) APC	eBioscience	Cat# 17-7211-82; RRID: AB_2016709
Anti-mouse IL-21 (149204) PE	R&D	Cat# IC594P; RRID: AB_2123982
Anti-mouse IL-22 (Poly5164) PE	BioLegend	Cat# 516404; RRID: AB_2124255
Anti-mouse IFN-γ (XMG1.2) BV421	BioLegend	Cat# 505830; RRID: AB_10897937
Anti-mouse IFN-γ (XMG1.2) PE-C7	BD Biosciences	Cat# 557649; RRID: AB_396766
MHC II-HBcAg128-140-Tetramer PE	NIH	N/A
Anti-human CD3 (UCHT1) PE	BioLegend	Cat# 300408; RRID: AB_2562047
Anti-human CD4 (OKT4) PE-CY7	BioLegend	Cat# 317414; RRID: AB_571958
Anti-human IFN-γ (4S.B3) FITC	BioLegend	Cat# 502506; RRID: AB_315230
Fixable Viability Stain 780	BD Biosciences	Cat# 565388; RRID: AB_2869673
Bacterial and virus strains		
Live Combined *Bifidobacterium*, *Lactobacillus* and *Enterococcus* Capsules	SINE	S10950032
Biological samples		
Human blood samples	This paper	N/A
Chemicals, peptides, and recombinant proteins		
Anti-CD3 mAb	BioXCell	Cat# BE0001-1; RRID: AB_1107634
Anti-CD4 mAb	BioXCell	Cat# BE0003-3; RRID: AB_1107642
Anti-CD8 mAb	BioXCell	Cat# BE0004-1; RRID: AB_1107671
Anti-TCRγ/δ mAb	BioXCell	Cat# BE0070; RRID: AB_1107751
Anti asialo GM1	Wako	Cat# 986-10001; RRID: AB_516844
Anti-IFN-γ mAb	BioXCell	Cat# BE0055; RRID: AB_1107694

(*Continued on next page*)

Continued

REAGENT or RESOURCE	SOURCE	IDENTIFIER
Anti-IL-21R mAb	BioXCell	Cat# BE0258; RRID: AB_2687737
Polyclonal Armenian hamster IgG	BioXCell	Cat# BE0091; RRID: AB_1107773
rat IgG2a isotype control	BioXCell	Cat# BE0089; RRID: AB_1107769
rat IgG1 isotype control	BioXCell	Cat# BE0290; RRID: AB_2687813
TRIzol universal reagent	TIANGEN	Cat# DP424
Phorbol 12-myristate 13-acetate (PMA)	Sigma-Aldrich	Cat# 79346
Ionomycin calcium salt	PeproTech	Cat# 5608212
$OVA_{323-339}$ peptide	AnaSpec	Cat# AS-27024
Spermidine	Sigma	Cat# S0266-5G
3-Methyladenine (3-MA)	MCE	Cat# HY-19312
GC-7	MCE	Cat# HY-108314A
Entecavir	MCE	Cat# HY-13623A
Critical commercial assays		
HBsAg ELISA Kits	InTec	S10910148
HBsAb ELISA Kits	InTec	20173400063
HBV DNA Kits	Sansure Biotech	20193400886
RevertAid First Strand cDNA Synthesis Kits	Thermo Scientific	Cat# K1622
Mouse IL-17A ELISA Kits	DAKEWEI	Cat# 1211702
Mouse IL-22 ELISA Kits	DAKEWEI	Cat# 1212202
Mouse IL-21 ELISA Kits	eBioscience	Cat# BMS6021
Mouse IFN-γ ELISA Kits	DAKEWEI	Cat# 1210002
Mouse iFABP ELISA Kits	J&L Biological	Cat# JL11487
ALT Assay Kits	Nanjing Jiancheng Bioengineering Institute	Cat# C009-2
AST Assay Kits	Nanjing Jiancheng Bioengineering Institute	Cat# C010-2
NucleoBond® Xtra Midi EF Kits	MACHEREY-NAGEL	Cat# 740420.50
CYTO-ID Autophagy Detection Kits	Enzo	Cat# ENA-51031
QIAamp Fast DNA Stool Mini Kits	Qiagen	Cat# DP328-02
Biotin Northern Blot Kits	Beyotime	Cat# R0219
Chemiluminescent Biotin-labeled Nucleic Acid Detection Kits	Beyotime	Cat# D3106
Deposited data		
16S rRNA sequencing dataset	National Center for Biotechnology Information (NCBI)	BioProject accession number SRA: PRJNA700493
Metabolomics dataset	National Metabolomics Data Repository (NMDR)	Study ID: ST003536
Experimental models: Organisms/strains		
OT-II TCR transgenic mice	Gift from Prof. Hua Tang (Shandong First Medical University)	N/A
C57BL/6JGpt (Germ-Free)	GemPharmatech Company	Cat# N000295
Oligonucleotides		
qPCR primer sequences, see Table S5	This paper	N/A
HBc probe 5′-AAGAAGAACTCCCTCGCCT CGCAGACG-3′	Beijing Tsingke Biotech Co., Ltd.	N/A
Recombinant DNA		
pAAV/HBV1.2	Gift from Prof. Zhepei Chen and Prof. Dingxin Chen (National Taiwan University)	N/A

(*Continued on next page*)

Continued

REAGENT or RESOURCE	SOURCE	IDENTIFIER
Software and algorithms		
GraphPad Prism	Graphpad Software	N/A
CytExpert Software	Beckman	Cytoflex
FlowJo 10.8.1.	FlowJo, LLC	N/A
EmpowerStat software (version 4.2)	EmpowerStat	N/A
Other		
Percoll	GE Healthcare	Cat# 17-0891-09
Collagenase IV	Worthington	Cat# LS004189
DNase I	Thermo	Cat# EN0521
Brefeldin A solution (1000×)	BioLegend	Cat# 420601
Fluorescein isothiocyanate-dextran	Sigma-Aldrich	Cat# 46944
Vancomycin	Solarbio	Cat# V8050
Neomycin Sulfate	Solarbio	Cat# N8090
Ampicilin	Solarbio	Cat# A8180
Metronidazole	Solarbio	Cat# M8060
MojoSort^{TM} buffer (5×)	BioLegend	Cat# 480017
IC Fixation Buffer	eBioscience	Cat# 00-8222-49
Permeabilization Buffer 10×	eBioscience	Cat# 00-8333-56
Intracellular Fixation & Permeabilization Buffer Set	eBioscience	Cat# 88-8824-00

EXPERIMENTAL MODEL AND STUDY PARTICIPANT DETAILS

Mice

WT C57BL/6 mice were purchased from Beijing Vital River Laboratory Animal Technology Company (Beijing, China). Germ-free mice were purchased from GemPharmatech Company (Jiangsu, China). OT-II TCR transgenic mice were kindly provided by Prof. Hua Tang (Shandong First Medical University). Specific-pathogen-free animals were bred in the specific-pathogen-free facility, and germ-free mice were bred in the sterile animal isolation facility in the Model Animal Research Center of Shandong University. All animal experiments were approved by the Animal Care and Use Committee of Shandong University (ECSBMSSDU2018-2-031).

Plasmids

HBV expression plasmids AAV/HBV1.2 were purified using a NucleoBond Xtra Midi EF kit (MACHEREY-NAGEL GmbH & Co. KG, Germany) according to the manufacturer's instructions.

HBV mouse model

To establish the HBV-carrier mouse model, 5-week-old male mice were hydrodynamically injected with 6 μg AAV/HBV1.2 plasmids within 5–8 s in a volume of phosphate-buffered saline (PBS) equivalent to 10% of the body weight. Mice were age-matched for individual experiments, and were regrouped according to serum HBsAg level at 3dpi after HDI to assure that there was no significant difference in HBsAg between the control and experimental groups before treatment. Then, serum was collected weekly to determine HBsAg and HBV DNA.

Probiotics, spermidine and entecavir administration

Bifico capsules are composed of $>1\times10^7$ colony forming units (CFUs) of live *Bifidobacterium*, *Lactobacillus* and *Enterococcus* (BLE) purchased from drugstores. Mice were gavage fed with 1-2 × 10^6 CFU of bacteria (BLE) daily starting two weeks before or at the same time of HDI. For oral SPD treatments, mice were fed with water containing 3 mM spermidine.[53] In combination therapy experiments, mice were gavage fed with a dose of entecavir at 0.1 mg/kg body weight and SPD daily 3 days after HDI.

Fecal microbiota transplantation

For ablation of intestinal bacteria in 3-week-old mice, an antibiotic cocktail of ampicillin (1 g/L, Solarbio), neomycin (1 g/L, Solarbio), metronidazole (1 g/L, Solarbio), and vancomycin (0.5 g/L, Solarbio) were used. Antibiotics were added to the drinking water every 3 days. Animals were administered with antibiotics for 2 weeks and switched to water without antibiotics two days before FMT.

To construct human flora-associated (HFA) mice, fecal microbiota was collected from CHB patients. Germ-free (GF) mice were gavage fed with fecal microbiota daily for 3 weeks, and then were hydrodynamically injected with AAV/HBV1.2.

Patients

We performed a preliminary observational study (NCT06313255) to explore the potential effects of BLE on anti-HBV treatment. Because BLE is commonly used for intestinal homeostasis for human bodies, there are parts of patients with chronic hepatitis B receiving treatment with BLE and antiviral drugs. Following comprehensive communication between physicians and patients, 10 patients volunteered to join the BLE group and received BLE supplements in combination with previously used antiviral treatments including nucleos(t)ide analogues or PegIFNα2b. As the Control group, the well gender- and age-matched 10 patients were enrolled and followed up using previous antiviral treatment without BLE supplement. The characteristics and treatment details of the included patients have been listed in the Tables S2 and S3.

We calculated the statistical power of the non-parametric Wilcoxon-Mann-Whitney test (for two groups) using EmpowerStat software (version 4.2) with current sample size (www.empowerstats.net, X&Y solutions, Inc. Boston, Massachusetts). With the α level set at 0.05, the statistical power for the composite of decline of HBsAg level (Control 10 vs. BLE group 10) was found to be 0.674, respectively. The study was approved by the Clinic Institutional Ethics Committee of Qilu Hospital of Shandong University (approval number: KYLL-202301-008-1) and was conducted in compliance with the principles of the Declaration of Helsinki. All patients provided written informed consent.

METHOD DETAILS

FITC-dextran administration and *In vivo* neutralization

To evaluate the gut permeability, mice were gavage fed with FITC-Dextran (4kDa, Sigma-Aldrich), and serum FITC fluorescence was detected 4 h later. To deplete specific immune cell subsets or block IFN-γ/IL-21 signaling, mice were injected intraperitoneally with 100 mg neutralization antibodies or isotype every 3 days from 0 to 6 wpi. Anti-CD4, anti-CD8, anti-TCRγ/δ, anti-IL-21R and anti-IFN-γ mAbs and their IgG isotype controls were purchased from Bio X Cell, and AsGM1 was purchased from Wako.

Enzyme-linked immunosorbent assays (ELISA)

IL-17A, IL-22, IL-21 or IFN-γ levels in tissue homogenates were determined with ELISA kits from DAKEWE (Shenzhen, China) or eBioscience according to the manufacturer's instructions. Serum levels of iFABP were determined with an ELISA kit from Jianglaibio (Shanghai, China) according to the manufacturer's instructions.

Quantitative real-time PCR

Total RNA from the small intestine and liver were isolated using Trizol (TIANGEN) and reverse transcribed into cDNA using Kit (Thermo Fisher Scientific). Gene expression was analyzed by SYBR Green real-time PCR (Bio-Rad) using primers for *β-actin, Occludin, Claudin1, Tjp1, Il17a, Il17f, Il21, Il22, Ifng, Il12, Tgfb, Eomes, Tbx21, Foxp3, Rorc, Bcl6.* Primer sequences are provided in Table S5.

Bacterial genomic DNA was extracted from fecal using QIAamp Fast DNA Stool Mini Kit (Qiagen, California, USA) according to the manufacturer's protocol. The bacterium-specific primers used to detect *B. longum*, *L. acidophilus* and *E. faecalis* were based on 16S rDNA gene sequences. *B. longum*, *L. acidophilus* and *E. faecalis* was isolated from BLE and was extracted genomic DNA to construct the standard curve. The cycle threshold of each sample was then compared with a homologous standard curve. The data are expressed as nanogram of *B. longum*, *L. acidophilus* and *E. faecalis* DNA per gram of feces. Primer sequences are provided in Table S5.

Quantitation of HBV replication

Serum HBsAg and HBsAb were analyzed using the ELISA kit following the manufacturer's instructions (InTec Inc., China). To ensure the OD value of serum HBsAg in the standard curve interval, the serum was properly diluted with PBS, and 100 μL of diluted samples were used for the assay. Serum HBV DNA were detected using commercial Sansure HBV DNA quantitation detection kit (Sansure Biotech, China). Total RNA was extracted from liver tissues and treated with DNase I (Thermo), and reverse transcribed into cDNA. The pgRNA levels were detected by qPCR with specific primers.

Northern blot

Total RNAs were isolated from liver tissues using TRIzol reagent (TIANGEN). For northern blot, the Biotin Northern Blot Kit (Beyotime, China) were used. HBc probes for northern blot were achieved using the Biotin 3′ End DNA Labeling Kit (Beyotime, China). Briefly, The RNA samples (15 μg) were separated by electrophoresis and were transferred to nylon membrane, which were then incubated with the hybridization solution containing the HBc probes. Finally, the RNA signal was detected using the Chemiluminescent Biotin-labeled Nucleic Acid Detection Kit (Beyotime, China). HBc probe sequence is provided in key resources table.

Cell isolation and culture

Small intestines were washed in stripping solution (PBS containing 1% EDTA and 2% FBS) at 37°C for 40 min to remove epithelial cells. Tissues were washed with ice-cold PBS, prior to enzymatic digestion in RPMI-1640 medium containing 1 mg/mL collagenase

IV (Worthington) and 60 μg/mL DNase I (Thermo). Digested material was passed through a cell strainer and separated on a discontinuous 40%/75% Percoll gradient. PP and mLN cells were isolated by mechanical grinding using frosted glass slides. The livers were pressed through a 200-gauge mesh. Liver mononuclear cells were prepared by lysing the erythrocytes with red cell lysis buffer and collected following 40% percoll density gradient centrifugation. The spleens were also pressed through a 200-gauge mesh and subjected to red cell lysis buffer prior to washing in ice-cold PBS for culture.

For *in vitro* cell culture, splenocytes from OT-II mice were stimulated with 2 μg/mL $OVA_{323-339}$ peptide and cultured in RPMI 1640 media supplemented with 10% FCS, 2 mM L-glutamine, 100 U/mL penicillin/streptomycin, 100 U/mL IL-2, 55 mM β-mercaptoethanol in 12-well plates at a seeding concentration of 3×10^6 cells per well for 3 days. Cells were collected and treated with SPD and indicated drugs in 48-well plates at a seeding concentration of 1×10^6 cells per well for 24 h. The following drugs were used: 2.5 μM, 5 μM, and 10 μM SPD (Sigma), 1 mM 3-MA (MCE) or 10 μM GC-7 (MCE).

Flow cytometry

The detailed information of antibodies for FCM analysis is listed in key resources table. For intracellular cytokine staining, cells were stimulated with 50 ng/mL PMA (Sigma-Aldrich) and 1 μg/mL ionomycin (PeproTech) for 5 h, and 1 × BFA (Biolegend, 1000 ×) was added after 1 h of PMA/ionomycin stimulation. After surface staining, cells were fixed and permeablized before intracellular staining using antibodies against IL-22, IL-17A, IL-21, and IFN-γ. Cells were stained with an antibody to Foxp3, T-bet and RORγt according to the manufacturer's protocol (eBioscience). Autophagy was measured using flow cytometry by quantifying autophagosome mean fluorescence intensity using the CYTO-ID Autophagy Detection Kit (Enzo, USA) according to the manufacturer's instructions and always following cell surface antibody staining. All data were collected using a flow cytometer (CytoFLEX S; Beckman Coulter) and analyzed with CytExpert software (Beckman Coulter, USA).

MHC class II tetramer

MHC class II tetramer was obtained from the National Institute of Health (NIH) Tetramer Core Facility (Atlanta, USA). Tetramer was labeled with $HBcAg_{128-140}$ peptide (TPPAYRPPNAPIL) and phycoerythrin. IA(b) human $CLIP_{87-101}$ peptide (PVSKMRMATPLLMQA) was used as the control reagent. To evaluate HBV-specific $CD4^+$ T cells, hepatic or splenic mononuclear cells were incubated with 6 μg/mL tetramer at 37°C for 1 h in PBS. The cells were then washed and stained for CD3, CD4 and IFN-γ.

16S rRNA sequencing

16S rRNA sequencing was performed by Majorbio Bio-pharm Company (Shanghai, China). Briefly, bacterial genomic DNA was extracted from fecal using QIAamp Fast DNA Stool Mini Kit (Qiagen, California, USA) according to the manufacturer's protocol. The V3-V4 hypervariable regions of the bacteria 16S rRNA gene were amplified by PCR with barcode-indexed primers 338F and 806R. The purified and quantified amplicons were paired-end sequenced on an Illumina MiSeq platform (Illumina, San Diego, California, USA). 16S rRNA sequencing data were deposited in NCBI (BioProject ID: PRJNA700493). The 16S rRNA sequencing data were analyzed using the Majorbio Cloud Platform. Operational taxonomic units (OTUs) were picked at 97% similarity cut-off, and the identified taxonomy was then aligned using the Silva database. After filtering, an average of 92 105 reads per sample was obtained (min: 51 258; max: 132 952). Alpha diversity was assessed using the species richness indices (Chao). Beta diversity was estimated by principal coordinates analysis (PCoA). The metagenomes of gut microbiome were imputed from 16S rRNA sequences with Linear Discriminant Analysis (LDA) Effect Size (LEfSe) and PICRUSt (Phylogenetic Investigation of Communities by Reconstruction of Unobserved States).

Metabolomics

Untargeted metabolomics was performed at Biotree Biotech Company (Shanghai, China) on fecal samples using a gas chromatograph system coupled with a Pegasus HT time-of-flight mass spectrometer (GC-TOF-MS) to detect primary metabolites. Briefly, fecal samples (50 ± 1 mg) were homogenized in 0.3 mL extraction liquid (Methanol: Chloroform = 3:1) with 20 μL of L-2-Chlorophenylalanine as internal standard. Supernatant (0.2 mL) was transferred to a fresh GC/MS glass vial, and 30 μL from each sample was pooled as the quality control sample. Samples and QCs were evaporated to dryness by vacuum concentrator and then derivatized with Methoxy amination hydrochloride (20 mg/mL in pyridine, and BSTFA +1% TMCS). GC-TOF-MS analysis was performed using an Agilent 7890 gas chromatograph system coupled with a Pegasus HT time-of-flight mass spectrometer. Chromatography was performed with a constant flow of 1 mL/min while increasing the oven temperature from 50°C to 310°C over a 26-min total run time. The mass spectrometry data were acquired in full-scan mode with the m/z range of 50–500 at a rate of 20 spectra per second after a solvent delay of 6.27 min. Chroma TOF 4.3X software of LECO Corporation and LECO-Fiehn Rtx5 database were used for analysis. The differential metabolites were imported to MetaboAnalyst 5.0 (https://www.metaboanalyst.ca), where Enrichment Analysis and Pathway Analysis were performed. Enrichment Ratio is computed by Hits/Expected, where hits = observed hits; expected = expected hits.

Polyamine concentrations in the liver were performed at Majorbio Bio-pharm Company (Shanghai, China) and determined by solvent extraction followed by gas chromatography-mass spectrometry (GC-MS). In short, samples were weighted and homogenized, and then the homogenate was transferred to an MCX SPE column. After sample adsorbing, the column was washed with 0.1 M HCl. Polyamines were eluted with methanol (v/v) containing 3% NH_4OH, and then blown to dryness by nitrogen. Samples and standards

were derivatized before analyzed by the Agilent 7820A-5977B GC-MS instrument (Agilent Technologies Inc. CA, UAS). In addition, spermidine concentrations in liver and feces from GF mice were performed at Sanshubio Company (Jiangsu, China) and determined by solvent extraction followed by liquid chromatography-mass spectrometry (LC-MS).

Evaluation of SPD in culture of BLE or *Enterococcus faecalis*

E. faecalis was separated from BLE. BLE or *E. faecalis* were each precultured in gifu anaerobe medium (GAM) at 37°C for 24 h, and then were inoculated at a final optical density at 600 nm (OD600) of 1.0×10^{-2} in GAM broth containing 2 mM L-arginine with different pH values (pH 5.0 or 7.0). After 24 h of culture, supernatants were collected by centrifugation (9100 g, 10 min), and the SPD concentration was measured by targeted metabolomics (Sanshubio Company, China, Shanghai).

Statistical analysis

Data were analyzed using Prism software (GraphPad, version 8). Data were presented as mean ± SEM, and *p* values were determined by two-tailed Student's t test, two-way analysis of variance (ANOVA). two-way ANOVA was followed up by Dunnett's multiple comparisons test for post hoc test. *0.01 < *p* value <0.05; **0.001 < *p* value <0.01; *** 0.0001 < *p* value <0.001; ****p value <0.0001. *p* value < 0.05 was considered as significant.